JEM Journal of Experimental Medicine

ARTICLE

Inborn errors of TLR3- or MDA5-dependent type I IFN immunity in children with enterovirus rhombencephalitis

Jie Chen[1,2], Huie Jing[3], Andrea Martin-Nalda[4,5,6], Paul Bastard[1,7,8], Jacques G. Rivière[4,5,6], Zhiyong Liu[1], Roger Colobran[6,9,10], Danyel Lee[1,7,8], Wesley Tung[3], Jeremy Manry[7,8], Mary Hasek[1], Soraya Boucherit[7,8], Lazaro Lorenzo[7,8], Flore Rozenberg[11], Mélodie Aubart[7,8,12], Laurent Abel[1,7,8*], Helen C. Su[3*], Pere Soler Palacin[4,5,6*], Jean-Laurent Casanova[1,7,8,13**], and Shen-Ying Zhang[1,7,8**]

Enterovirus **(EV) infection rarely results in life-threatening infection of the central nervous system. We report two unrelated children with EV30 and EV71 rhombencephalitis. One patient carries compound heterozygous *TLR3* variants (loss-of-function F322fs2* and hypomorphic D280N), and the other is homozygous for an *IFIH1* variant (loss-of-function c.1641+1G>C). Their fibroblasts respond poorly to extracellular (TLR3) or intracellular (MDA5) poly(I:C) stimulation. The baseline (TLR3) and EV-responsive (MDA5) levels of IFN-β in the patients' fibroblasts are low. EV growth is enhanced at early and late time points of infection in TLR3- and MDA5-deficient fibroblasts, respectively. Treatment with exogenous IFN-α2b before infection renders both cell lines resistant to EV30 and EV71, whereas post-infection treatment with IFN-α2b rescues viral susceptibility fully only in MDA5-deficient fibroblasts. Finally, the poly(I:C) and viral phenotypes of fibroblasts are rescued by the expression of WT TLR3 or MDA5. Human TLR3 and MDA5 are critical for cell-intrinsic immunity to EV, via the control of baseline and virus-induced type I IFN production, respectively.**

Introduction

Enterovirus (EV) is a viral genus of positive-sense single-stranded RNA viruses belonging to the family Picornaviridae that commonly causes disease in children (de Crom et al., 2016; Moore, 1982). There are 81 nonpoliovirus and 3 poliovirus types of EV (de Crom et al., 2016). Echovirus 30 (EV30) is one of the most frequently isolated EVs, causing outbreaks of meningitis in European countries, whereas EV71 causes outbreaks of hand, foot, and mouth disease (HFMD) every spring, mostly in eastern Asia (Shih et al., 2000; Cabrerizo et al., 2008; Lévêque et al., 2010; Trallero et al., 2010; Wu et al., 2010; Zeng et al., 2012; Thoa et al., 2013; Rudolph et al., 2017). Since 2000, outbreaks of EV71 (and EV68) disease have been reported in various countries and continents (Chan et al., 2000; McMinn et al., 2001; Fowlkes et al., 2008; Mirand et al., 2010; Meijer et al., 2012; Xiang et al., 2012; Andrés et al., 2019; Wörner et al., 2021). Poliovirus is a highly infectious and neurovirulent EV that causes paralytic poliomyelitis in rare cases (<1% of those infected; Mehndiratta et al., 2014). An efficient global vaccination campaign has resulted in its near eradication. Over 90% of people infected with nonpoliovirus EVs remain asymptomatic, or have only mild clinical manifestations, such as fever, runny nose, skin rash, and mouth blisters. However, a small proportion of infected

[1]St. Giles Laboratory of Human Genetics of Infectious Diseases, Rockefeller Branch, The Rockefeller University, New York, NY; [2]Department of Infectious Diseases, Shanghai Sixth Hospital, Shanghai Jiaotong University, Shanghai, China; [3]Laboratory of Clinical Immunology and Microbiology, Intramural Research Program, National Institute of Allergy and Infectious Diseases, National Institutes of Health, Bethesda, MD; [4]Infection in Immunocompromised Pediatric Patients Research Group, Vall d'Hebron Research Institute, Vall d'Hebron University Hospital, Vall d'Hebron Barcelona Hospital Campus, Barcelona, Spain; [5]Pediatric Infectious Diseases and Immunodeficiencies Unit, Vall d'Hebron University Hospital, Vall d'Hebron Barcelona Hospital Campus, Barcelona, Spain; [6]Jeffrey Modell Diagnostic and Research Center for Primary Immunodeficiencies, Barcelona, Spain; [7]Laboratory of Human Genetics of Infectious Diseases, Necker Branch, Institut National de la Santé et de la Recherche Médicale U1163, Paris, France; [8]University of Paris, Imagine Institute, Paris, France; [9]Diagnostic Immunology Group, Vall d'Hebron Research Institute, Vall d'Hebron University Hospital, Vall d'Hebron Barcelona Hospital Campus, Barcelona, Spain; [10]Immunology Division, Genetics Department, Vall d'Hebron University Hospital, Vall d'Hebron Barcelona Hospital Campus, Universitat Autònoma de Barcelona, Barcelona, Spain; [11]Laboratory of Virology, Assistance Publique-Hôpitaux de Paris, Cochin Hospital, Paris, France; [12]Pediatric Neurology Department, Necker-Enfants Malades Hospital, Assistance Publique-Hôpitaux de Paris, Paris, France; [13]Howard Hughes Medical Institute, New York, NY.

*L. Abel, H.C. Su, and P. Soler Palacin contributed equally to this paper; **J.-L. Casanova and S.-Y. Zhang contributed equally to this paper; Correspondence to Shen-Ying Zhang: shzh289@rockefeller.edu; Jean-Laurent Casanova: casanova@rockefeller.edu.

individuals, especially young children, develop severe complications that can be life-threatening, such as myocarditis, myelitis, and encephalitis (Abzug et al., 2003; Antona et al., 2016; Aubart et al., 2020). EV may enter the central nervous system (CNS) via neuronal or hematogenous routes, crossing the blood-brain barrier (Chen et al., 2007; Ong et al., 2008; Yang et al., 1997), and resulting in meningitis or encephalitis, which typically presents as rhombencephalitis, affecting the brainstem and cerebellum (Chang et al., 2019; Huang et al., 1999; Jubelt and Lipton, 2014). During an EV71 outbreak in Taiwan in 1998, 0.05% of those infected developed encephalitis (Lin et al., 2002). In addition to EV30, EV71, and EV68, many other nonpoliovirus EVs, such as coxsackieviruses A9, A10, and B5, echoviruses 4, 5, 9, 11, and 19, and EV75, 76, and 89, have been identified in patients with encephalitis (Chen et al., 2020; Dalwai et al., 2009; Fowlkes et al., 2008; Kumar et al., 2011; Lewthwaite et al., 2010; Lin et al., 2003). More than 70% of patients with EV encephalitis (EVE) are <19 yr old (Fowlkes et al., 2008). The causal virus has been identified (Chen et al., 2020), but the pathogenesis of EVE remains otherwise unknown.

Severe and chronic EV infection has been observed in rare patients with X-linked agammaglobulinemia (XLA) and other profound inherited antibody deficiencies (Dropulic and Cohen, 2011). These patients also typically have severe infections due to various other viral, bacterial, and parasitic pathogens (Bearden et al., 2016; Jones et al., 2019; Winkelstein et al., 2006). EV meningoencephalitis may affect as many as 7% of XLA patients. These genetic defects are causal for EV infection of the CNS in the affected patients, via molecular and cellular mechanisms probably involving inadequate antibody-mediated EV neutralization. Furthermore, EV encephalomyelitis, leading to a fatal neurodegenerative condition, has been observed in a patient with a heterozygous mutation of *NFKB2* who was diagnosed with "possible common variable immunodeficiency," and who also showed failure to thrive, recurrent lower respiratory tract infections, and widespread molluscum contagiosum (Slade et al., 2019). The mechanism of EV disease has yet to be determined in this patient with multiple clinical phenotypes. The immunopathogenesis underlying severe EV disease in otherwise healthy patients suffering from isolated EVE is also completely unknown. Previous studies by our group and others have provided evidence that various monogenic inborn errors impairing CNS cell-intrinsic antiviral immunity, via known type I IFN–mediated (mutations affecting the TLR3-dependent type I IFN circuit) or previously unknown (mutations of *SNORA31* or *DBR1*) molecular mechanisms, can underlie encephalitis due to HSV-1, influenza virus, or norovirus in otherwise healthy children (Andersen et al., 2015; Casrouge et al., 2006; Guo et al., 2011; Herman et al., 2012; Lafaille et al., 2019; Lim et al., 2014; Pérez de Diego et al., 2010; Sancho-Shimizu et al., 2011; Zhang, 2020; Zhang and Casanova, 2015; Zhang et al., 2018; Zhang et al., 2007). Mutations of other genes have been shown to underlie Mollaret's HSV–meningitis (Tang et al., 2000). Here, we tested the hypothesis that EVE may result from rare single-gene inborn errors of immunity affecting cell-intrinsic type I IFN–mediated antiviral mechanisms in the CNS, at least in some otherwise healthy children.

Results

Two children with EV rhombencephalitis

We performed trio whole exome sequencing (WES; the patient and both parents) for a cohort of 15 unrelated children with EV rhombencephalitis. We focused on two patients with obvious candidate genetic lesions. Patient 1 (P1; Fig. 1 A) was a boy born to nonconsanguineous parents of sub-Saharan African origin living in Spain. He was healthy until the age of 3.5 yr, when he developed fever, vomiting, drowsiness, and stiff neck. Meningoencephalitis was suspected. PCR tests for EV30 on cerebrospinal fluid, stool, and respiratory samples gave positive results. A brain electroencephalogram suggested diffuse nonspecific neurological dysfunction without paroxysms. Brain magnetic resonance imaging showed pathological tegmental hypersignal without evidence of diffusion restriction associated with cervical myelitis, highly suggestive of rhombencephalitis (Fig. 1 B and Fig. S1 A). After supportive treatment, the patient's clinical condition improved, and he was discharged 3 d after admission, without sequelae. P2 was a boy born to nonconsanguineous Spanish parents (Fig. 1 A). He was healthy and had not suffered from other unusually severe infectious diseases, including those of viral origin, until he developed EV71 encephalitis at the age of 12 mo. He was admitted to the intensive care unit for fever, HFMD, shallow irregular breathing, somnolence, apnea, and ataxia. EV71 PCR was positive for respiratory and stool samples, but negative for a cerebrospinal fluid sample. Brain electroencephalogram showed diffuse neurological dysfunction. A pathological tegmental hypersignal was observed on brain magnetic resonance imaging, with evidence of diffusion restriction in the superior cerebellar peduncles and ponto-bulbar junction associated with cervical myelitis, which was highly suggestive of rhombencephalitis (Fig. 1 B and Fig. S1 A). The child was diagnosed with rhombencephalitis associated with HFMD and was treated with intravenous immunoglobulin therapy and methylprednisolone. He recovered and was discharged from the hospital with mild dysphagia and aphonia. P1 is now 8 yr old, and P2 is 5 yr old. Neither has suffered any other severe infectious disease since hospitalization for EVE. Serological tests showed that both patients currently have antibodies against HSV-1 and other viruses (Fig. S1 B), suggesting past infection with these viruses without severe clinical consequences.

The two patients carry biallelic mutations of *TLR3* or *IFIH1*

We searched the WES data of 15 EVE patients for relatively rare (minor allele frequency [MAF] <0.01 in the Genome Aggregation Database [gnomAD] and in our in-house WES database containing ~10,000 exomes) nonsynonymous variants with a combined annotation-dependent depletion (CADD) score >10, in genes related to type I IFN immunity and previously shown to underlie other severe viral infections in humans (Casanova and Abel, 2020), with an autosomal recessive (AR) mode of inheritance. We excluded variants of genes with a gene damage index >13.83, the gene damage index cutoff for AR human disease-causing gene prediction (Itan et al., 2015). The trio WES design made it possible for us to select homozygous or compound-heterozygous variants with full penetrance (Casanova et al., 2014). Our analyses revealed two compound-heterozygous variants

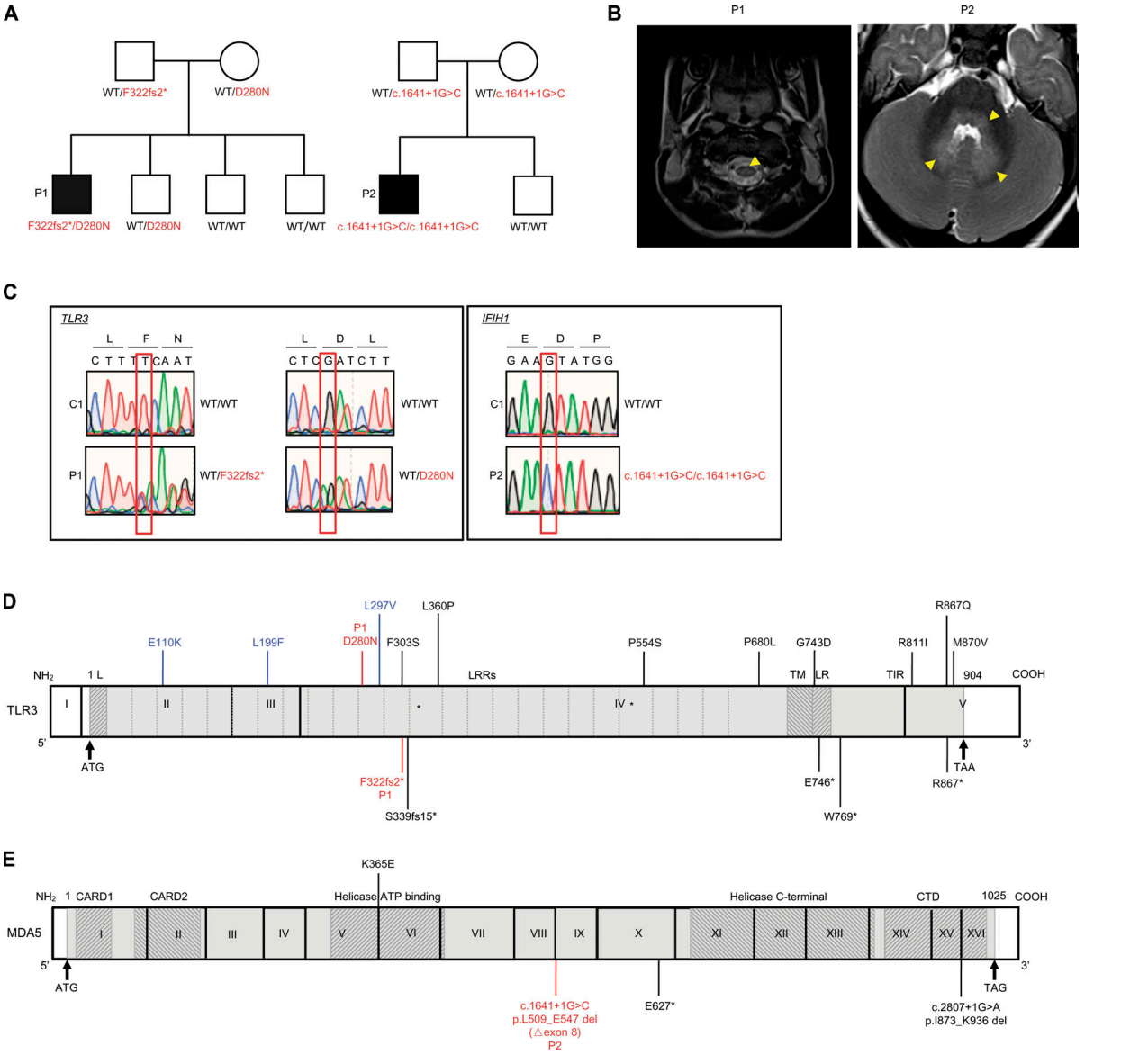

Figure 1. **Biallelic *TLR3* or *IFIH1* mutations in two patients with EVE. (A)** Family pedigrees, showing segregation of the *TLR3* and *IFIH1* mutations. The black symbols indicate patients. **(B)** Brain imaging showing EVE lesions in P1 and P2. In P1, post-contrast T1-FLAIR imaging showed pathological tegmental hypersignal (yellow arrows) associated with cervical myelitis, highly suggestive of rhombencephalitis. In P2, post-contrast T1-FLAIR imaging showed pathological tegmental hypersignal with evidence of diffusion restriction in the superior cerebellar peduncles and the ponto-bulbar junction (yellow arrows), suggestive of rhombencephalitis. **(C)** Confirmation of the mutations by Sanger sequencing. The single nucleotide substitutions for each patient relative to the sequence for a healthy control are indicated by red squares. **(D)** Schematic diagram of the structure of the human *TLR3* gene and protein, featuring the leader sequence (L), leucine-rich repeats (LRRs), transmembrane domain (TM), linker region (LR), and Toll/IL-1 receptor (TIR) domain. Roman numerals indicate the coding exons. Mutations previously identified in patients with HSE (E110K, L297V, L360P, P554S, G743D, E746*, R811I, R867Q), IAV or SARS-CoV-2 pneumonia (S339fs15*, P554S, P680L, W769*, M870V) or patients with other viral infections (F303S, L199F, R867*) are shown in black (experimentally characterized) or blue (not characterized). The mutations (D280N and F322fs2*) found in P1 are shown in red. **(E)** Schematic diagram of the structure of the human *IFIH1* gene and MDA5 protein, featuring the CARD domain, helicase ATP-binding domain, helicase C-terminal domain, and carboxy-terminal domain. Roman numerals indicate the coding exons. Mutations previously identified in patients with respiratory virus infections are shown in black. The mutation (c.1641+1G>C, p.L509_E547 del [▵exon8]) found in P2 is shown in red.

of *TLR3* in P1, and one homozygous variant of *IFIH1* in P2. TLR3 is a highly conserved endosomal receptor of double-stranded RNA (dsRNA; Alexopoulou et al., 2001; Mikami et al., 2012), and an inducer of antiviral IFN-α/β and -λ. AR or autosomal dominant (AD) TLR3 deficiency has been shown to underlie herpes simplex encephalitis (HSE), influenza A virus (IAV), and SARS-CoV-2 pneumonia, due to the impairment of cell-intrinsic antiviral immunity (Guo et al., 2011; Lim et al., 2014; Zhang et al., 2020; Zhang et al., 2007). P1 is compound heterozygous for a frameshift variant (c.965delT, p.F322fsTer2, referred to hereafter as F322fs2*) and a missense variant (c.838G>A, p.D280N; Fig. 1, A and C), both located in the ectodomain of TLR3, which plays an important role in ligand binding and receptor dimerization (Choe et al., 2005; Fig. 1 D). The F322fs2* variant is

private and was not found in any of the public databases (1000 Genomes, dbSNP, gnomAD, or Bravo) or in our in-house WES database. The D280N variant affects a residue that is conserved across ∼80% of the vertebrate species studied (Fig. S1 C). It has a CADD score of 14.47, a global MAF of 0.0017, and a MAF of 0.017 in the African population, with one homozygous carrier found in gnomAD. *IFIH1* encodes MDA5, a cytosolic receptor of dsRNA and inducer of antiviral IFN-α/β and -λ (Gitlin et al., 2006; Kang et al., 2002; Kato et al., 2006; Wu and Hur, 2015). AR or AD MDA5 deficiency is a known genetic etiology of rhinovirus pneumonia, and possibly other conditions caused by respiratory viruses (Asgari et al., 2017; Lamborn et al., 2017). P2 is homozygous for an essential splicing variant (c.1641+1G>C) of *IFIH1* (Fig. 1, A and C). This variant has a CADD score of 33, a global MAF of 0.0067, and a MAF of 0.01 in the European population, with seven homozygous carriers found in gnomAD. The cumulative frequency of homozygous carriers in the general population is therefore compatible with the prevalence of EVE. Furthermore, this variant has been previously shown, in assays performed in vitro, to result in abnormal splicing of the MDA5 mRNA (▵exon8) leading to the removal of 39 aa from the conserved helicase ATP-binding domain and linker region of the MDA5 protein (p.L509_E547 del; Fig. 1 E), and a loss of function for IFN-β luciferase activity induction (Asgari et al., 2017; Lamborn et al., 2017). Finally, trio WES for the two families identified no other plausible candidate genes in the patients, related to type I IFN immunity or otherwise, in analyses of biallelic or de novo variants in the two patients (Table S1 and Table S2). We identified no rare nonsynonymous variants (MAF <0.01) of known inborn errors of immunity–causing genes, including the XLA-causing gene *BTK*. Sanger sequencing confirmed the *TLR3* and *IFIH1* variants in P1 and P2, respectively, and the patterns of segregation in the two families confirmed AR inheritance for both families (Fig. 1 A). Thus, the biallelic *TLR3* and *IFIH1* variants were considered to be candidate EVE-causing variants in the two patients.

Expression and function of the TLR3 variants of P1 in vitro

We tested the hypothesis that the compound heterozygous F322fs2* and D280N variants found in P1 resulted in AR TLR3 deficiency by investigating the production and function of the corresponding mutant proteins in a TLR3-deficient P2.1 fibrosarcoma cell line without detectable levels of TLR3 protein and that did not respond to the dsRNA mimic polyinosinic:polycytidylic acid (poly[I:C]). Following the stable transfection of P2.1 cells with constructs encoding C-terminally hemagglutinin (HA)–tagged WT, D280N, or F322fs2* TLR3, the levels of *TLR3* mRNA produced from the various constructs were similar (Fig. 2 A). The WT and D280N proteins were detected by Western blotting with an antibody against TLR3 or an antibody against HA, at molecular weights of ∼130 kD and ∼70 kD, corresponding to the full-length and C-terminally cleaved forms, respectively. By contrast, transfection with F322fs2* *TLR3* resulted in no detectable protein (Fig. 2 B), suggesting that the F322fs2* mutation destabilized the protein. We then studied the function of the two *TLR3* variants of P1 in the same cells, using cells stably expressing WT, W769*, or R867Q *TLR3* as controls, with these last two variants previously reported to be loss-of-function and hypomorphic (Lim et al., 2014; Zhang et al., 2020), respectively. The transfection of P2.1 cells with either the W769* or F322fs2* *TLR3* allele did not restore poly(I:C)-induced *IFNB* and *IFNL1* mRNA induction, whereas this induction was restored by transfection with WT *TLR3* (Fig. 2, C and D). R867Q had ∼50% the activity of WT *TLR3*, whereas D280N had ∼70% WT *TLR3* activity (Fig. 2, C and D; and Fig. S2). The F322fs2* *TLR3* mutant is, therefore, both loss-of-expression and loss-of-function, whereas the D280N mutant is normally expressed but mildly hypomorphic. The c.1641+1G>C *IFIH1* variant of P2 has been shown in vitro to result in completely abnormal splicing of the *IFIH1* mRNA, with the deletion of the entire coding sequence of exon8 (▵exon8, p. L509_E547 del). The encoded MDA5 protein has been shown to be loss-of-function for IFN-β luciferase activity induction (Asgari et al., 2017; Lamborn et al., 2017). Together, our new data and published findings for the *IFIH1* variant found in P2 suggest that compound heterozygosity for the two *TLR3* variants leads to AR partial TLR3 deficiency in P1, whereas homozygosity for the *IFIH1* variant leads to AR complete MDA5 deficiency in P2. These variants may underlie EVE by impairing the antiviral IFN-α/β and -λ immunity mediated by two different dsRNA-sensing pathways.

Impaired TLR3-dependent extracellular poly(I:C) responsiveness in the fibroblasts of P1

Human dermal fibroblasts express TLR3 and respond to extracellular poly(I:C) stimulation in a TLR3-dependent manner (Guo et al., 2011; Lim et al., 2019; Lim et al., 2014; Zhang et al., 2007). We investigated whether compound heterozygosity for the two *TLR3* variants impaired TLR3 responses in the cells of P1, by first quantifying the percentages of mRNA for the two variants in SV40-immortalized fibroblasts (SV40-fibroblasts) and primary fibroblasts from P1, by topoisomerase-based cloning (TOPO-TA cloning), and the sequencing of a *TLR3* cDNA generated by reverse transcription from the RNA in the cells of P1. Unlike cDNA from healthy control fibroblasts, which contained 100% WT *TLR3* sequences, 50.4% and 46.5% of the *TLR3* cDNA sequences carried the F322fs2* variant and 49.6% and 53.5% the D280N variant obtained from P1's SV40-fibroblasts and primary fibroblasts, respectively (Fig. 3 A). We then studied the response to exogenous poly(I:C) stimulation in SV40-fibroblasts from P1, comparing our findings with those for cells from three healthy controls, an HSE patient with AD TLR3 deficiency by haploinsufficiency (due to heterozygous G743D+R811I mutations), an HSE patient with AD TLR3 deficiency by negative dominance (due to heterozygous P554S), and an HSE patient with AR complete TLR3 deficiency (*TLR3*$^{-/-}$, due to compound heterozygous P554S and E746* mutations; Guo et al., 2011; Lim et al., 2014; Zhang et al., 2007). After 24 h of stimulation with various concentrations of poly(I:C), the secretion of the IFN-β, IFN-λ, and IL-6 proteins was severely impaired in P1's SV40-fibroblasts upon different doses of poly(I:C) stimulation, similar to P554S/WT, G743D+R811I/WT, and *TLR3*$^{-/-}$ fibroblasts from various HSE patients, but unlike SV40-fibroblasts of three healthy controls, which displayed dose-dependent responses (Fig. 3 B). We also assessed the production of *IFNB* and *IFNL1* mRNA, by

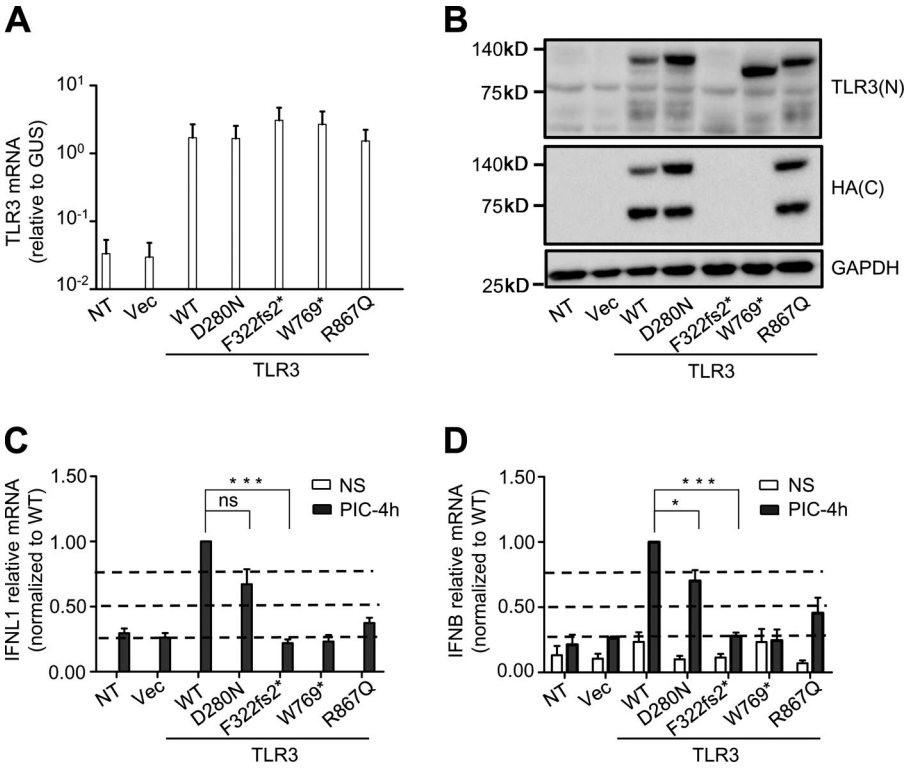

Figure 2. **Production and function of the mutant forms of TLR3 of P1 in vitro. (A)** *TLR3* mRNA levels were determined by RT-qPCR in P2.1 TLR3-deficient fibrosarcoma cells, without transfection, or after transfection with an empty vector (Vec), HA-tagged *TLR3* WT, D280N, or F322fs2*. *TLR3* W769* and R867Q were used as experimentally confirmed loss-of-function or hypomorphic control mutants. **(B)** TLR3 was detected by immunoblotting. P2.1 cells, either untransfected (NT) or stably transfected with empty vector (Vec), HA-tagged WT or mutant *TLR3* were immunoblotted with a C-terminal (C) HA-specific antibody or N-terminal (N) TLR3-specific antibody. GAPDH was used as a loading control. **(C and D)** RT-qPCR for *IFNL1* (C) or *IFNB* (D) mRNA induction without stimulation (NS) or after 4 h of stimulation with 25 µg/ml poly(I:C) (PIC-4h) in P2.1 cells not transfected (NT) or stably transfected with empty vector (Vec), HA-tagged WT or mutant *TLR3*. **(A, C, and D)** Mean values ± SD were calculated from four independent experiments. P values were obtained by one-way ANOVA and subsequent Tamhane's T2's multiple comparison tests, and the respective P values are indicated. ns, P > 0.05; *, P < 0.05; ***, P < 0.001.

quantitative RT-PCR (RT-qPCR), in P1 and control SV40-fibroblasts after 4 h of poly(I:C) stimulation. We found that the induction of *IFNB* and *IFNL1* mRNA was severely impaired but not entirely abolished in P1's fibroblasts, consistent with severe but partial TLR3 deficiency (Fig. 3 C). By contrast, both the fibroblasts of P1 and those of other TLR3-deficient patients produced normal amounts of IFN-β and IFN-λ in response to Lipofectamine-mediated intracellular transfection with poly(I:C), resulting in stimulation activating RIG-I and MDA5 in the cytosol (Li et al., 2009; Fig. 3 B). All the cells produced high levels of *IFNB* and *IFNL1* in response to infection with vesicular stomatitis virus (VSV) M51R, which activates RIG-I (Fig. 3 C). Finally, the impaired poly(I:C) response of P1's fibroblasts was rescued by the stable expression of exogenous WT TLR3, but not of the D280N or F322fs2* mutants (Fig. 3, D–G). These results validate our hypothesis that compound heterozygosity for D280N and F322fs2* led to AR partial TLR3 deficiency at the cellular level in P1.

Impaired MDA5-dependent responsiveness to intracellular poly(I:C) in the fibroblasts of P2

MDA5 and RIG-I are cytosolic dsRNA receptors that produce antiviral IFN-α/β and -λ (Li et al., 2009). They sense long tracts of dsRNA and the 5′-tri-/di-phosphate ends of dsRNA, respectively (Reikine et al., 2014). We investigated whether homozygosity for the *IFIH1* c.1641+1G>C allele would lead to AR MDA5 deficiency at the cellular level, using SV40-fibroblasts from P2. We first generated a *IFIH1* cDNA from P2's fibroblasts, and amplified it by PCR, with primers spanning exons 6–10, resulting in a single product ∼117 bp smaller than that obtained from healthy control cells (Fig. 4 A). Consistent with previous reports for in vitro characterization of the c.1641+1G>C variant, Sanger sequencing of the PCR product confirmed a deletion of 117 bp corresponding to the entire exon 8 of *IFIH1* (Fig. 4 B). This deletion was predicted to remove 39 aa from the helicase ATP-binding domain and the linker region helicase C-terminal domain of the MDA5 protein (Fig. 1 E). TOPO-TA cloning and sequencing of the PCR product further confirmed that all the transcripts from P2's cells contained the ▵exon8 deletion, whereas healthy control cells contained only WT transcripts (Fig. 4 C). We then compared the levels of MDA5 mRNA and protein between SV40-fibroblasts from P2, SV40-fibroblasts from two healthy controls, and SV40-fibroblasts with a CRISPR/Cas9-mediated MDA5 KO. P2's SV40-fibroblasts contained smaller amounts of *IFIH1* mRNA than the cells from healthy controls, in analyses based on RT-qPCR with probes spanning exons 5–6, exons 8–9, or exons 9–10 of *IFIH1*, with this difference most pronounced for the probe spanning exons 8–9 (Fig. 4 D). MDA5 protein was detected in P2's SV40-fibroblasts, at a slightly lower molecular weight than the protein detected in control cells (Fig. 4 E), reflecting the deletion of 39 aa due to the ▵exon8 variant (Fig. 4 B). Levels of MDA5 protein were markedly lower in the SV40-fibroblasts of P2 than in those from healthy controls or TLR3-deficient patients (Fig. 4 E). Finally, following intracellular poly(I:C) stimulation mediated by electroporation, specifically activating the MDA5 pathway in human fibroblasts, we observed an impairment of *IFNB* expression in the primary fibroblasts of P2 relative to those of healthy controls (Fig. 4 F). By contrast, IFN-β induction levels were similar in the SV40-fibroblasts of P2 and healthy controls, following extracellular poly(I:C) stimulation, which activates the TLR3 pathway, intracellular T7-GFP, or 5′ppp-dsRNA stimulation, which

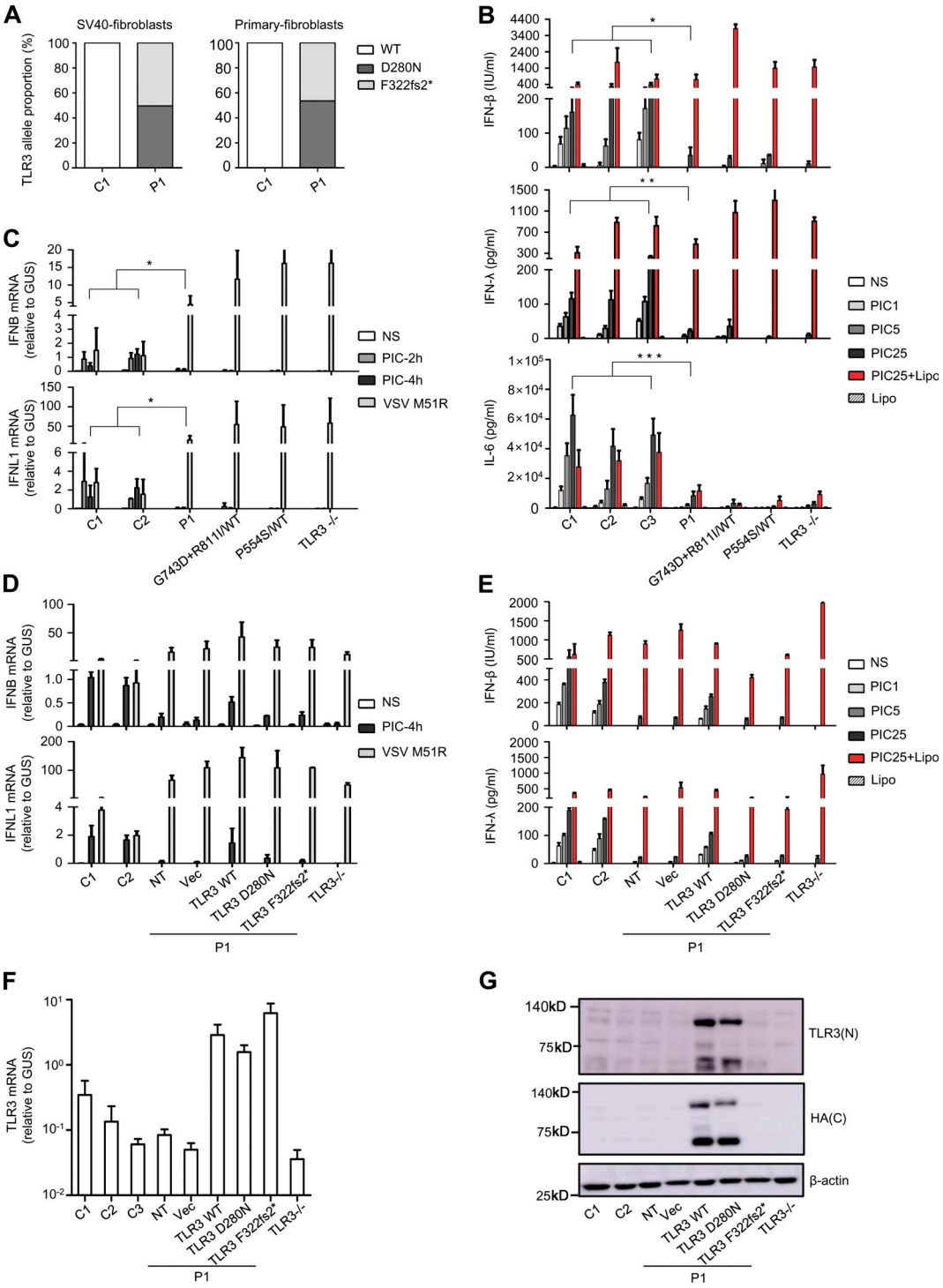

Figure 3. **Impairment of TLR3-dependent extracellular poly(I:C) responsiveness in P1's SV40-fibroblasts and rescue by WT TLR3. (A)** TOPO-TA cloning of *TLR3* cDNA from P1's SV40-fibroblasts and primary fibroblasts, and comparison with that from a healthy control. The percentage of the TLR3 sequences in cDNA clones from P1, 101 clones from SV40-fibroblasts, and 101 clones from primary fibroblasts that contained the D280N and F322fs2* mutations is shown, and compared with that for clones isolated in a similar manner from healthy control cells. **(B)** Production of IFN-β, IFN-λ, and IL-6 by SV40-fibroblasts from three healthy controls (C1, C2, C3), P1, TLR3 P554S/WT, TLR3 G743D+R811I/WT, or *TLR3*$^{-/-}$ patients, 24 h after stimulation with 1, 5, or 25 µg/ml poly(I:C) (PIC), and 25 µg/ml poly(I:C) in the presence of Lipofectamine (Lipo; PIC25+Lipo), or Lipo alone, as assessed by ELISA. **(C)** *IFNB* and *IFNL1* mRNA levels in SV40-fibroblasts from two controls (C1, C2), P1, TLR3 P554S/WT, TLR3 G743D+R811I/WT, or *TLR3*$^{-/-}$ patients, not stimulated (NS), stimulated for 2 and 4 h with 25 µg/ml poly(I:C), or infected with VSV M51R at an MOI of 1 for 18 h. GUS was included for normalization. **(D)** *IFNB* and *IFNL1* mRNA induction without stimulation (NS), after 4 h of stimulation with 25 µg/ml poly(I:C), or after 18 h of stimulation with VSV M51R, in SV40-fibroblasts from two controls (C1, C2) and P1, without plasmid transfection (NT) or after transfection with the empty vector (Vec) or with HA-tagged WT, D280N, or F322fs2* *TLR3*, and fibroblasts from a *TLR3*$^{-/-}$ patient. **(E)** Production of IFN-β and IFN-λ, in the absence of stimulation (NS), after 24 h of stimulation with 1, 5, or 25 µg/ml poly(I:C), and 25 µg/ml poly(I:C) with or without Lipo, as assessed by ELISA, in SV40-fibroblasts from two controls (C1, C2), from P1 with and without

transfection with various plasmids, as in D, and fibroblasts from a *TLR3*$^{-/-}$ patient. **(F)** *TLR3* mRNA levels were determined by RT-qPCR in SV40-fibroblast cells from controls (C1, C2, C3), or from P1 with or without transfection with various plasmids, as in D. **(G)** TLR3 expression was detected by immunoblotting, with an N-terminal (N) TLR3 antibody or C-terminal (C) HA antibody, in SV40-fibroblast cells from controls (C1, C2), or from P1 with or without transfection with various plasmids, as in D. β-actin was used as a loading control. Mean values ± SD were calculated from three (B–D and F) or two (E) independent experiments, with biological duplicates performed in each experiment. P values were obtained by Student's *t* test by comparing P1's fibroblasts with all control fibroblasts after 24 h of stimulation with 25 µg/ml poly(I:C) (B), or after 4 h of stimulation with 25 µg/ml poly(I:C) (C). *, P < 0.05; **, P < 0.01; ***, P < 0.001. The result shown in G is representative of that from three independent experiments.

activates the RIG-I pathway, or Lipofectamine-mediated high-dose poly(I:C) transfection, which activates both the RIG-I and MDA5 pathways under the testing conditions (Fig. 4, G and H). The stable transduction of P2's SV40-fibroblasts with WT *IFIH1* rescued the impaired responsiveness to electroporation-mediated intracellular poly(I:C) stimulation (Fig. 4, I and J). Thus, homozygosity for c.1641+1G>C *IFIH1* led to completely abnormal splicing and low levels of MDA5 expression, resulting in AR MDA5 deficiency at the cellular level. The deficiency is probably complete, as the ▵exon8 *IFIH1* mutation resulted in a complete loss of function in in vitro assays (Asgari et al., 2017; Lamborn et al., 2017).

Impaired basal or EV-induced IFN-β and -λ production in the patients' fibroblasts

TLR3 and MDA5 govern two spatially different IFN-α/β- or -λ–inducing dsRNA-sensing pathways, with TLR3 in the endosomal compartment and MDA5 in the cytoplasm (Kang et al., 2002; Krishnan et al., 2007). We have shown that inborn errors of TLR3 or MDA5 can underlie HSE, IAV pneumonia, SARS-CoV-2 pneumonia (Guo et al., 2011; Lim et al., 2019; Lim et al., 2014; Zhang et al., 2020; Zhang et al., 2007), and rhinovirus pneumonia, and possibly other severe diseases due to respiratory viral pathogens (Asgari et al., 2017; Lamborn et al., 2017). With this new discovery of a partial form of AR TLR3 deficiency and a complete form of AR MDA5 deficiency in EVE patients, we hypothesized that TLR3 and MDA5 deficiencies might impair either basal (TLR3; Gao et al., 2021) or virus-induced (MDA5) IFN-α/β or -λ production (Asgari et al., 2017; Lamborn et al., 2017; Slater et al., 2010; Wang et al., 2009), resulting in EVE through spatially and temporally different mechanisms. Indeed, the basal levels of *IFNB* and *IFNL1* mRNA were significantly lower in SV40-fibroblasts from P1 than in those of healthy controls, as for the SV40-fibroblasts of a *TLR3*$^{-/-}$ HSE patient (Fig. 5, A and B). However, the basal levels of *IFNB* and *IFNL1* mRNA in the SV40-fibroblasts of P2 and in MDA5 KO SV40-fibroblasts were similar to those in healthy control cells (*IFNB*) or were intermediate, lower than those in healthy control cells but higher than those in *TLR3*$^{-/-}$ SV40-fibroblasts (*IFNL1*; Fig. 5, A and B). We then studied the induction of IFN-α/β or -λ upon EV infection in TLR3- or MDA5-deficient fibroblasts. Like rhinoviruses, which trigger MDA5-dependent IFN induction (Slater et al., 2010; Wang et al., 2009), EV belongs to the picornavirus family (van der Linden et al., 2015). Following infection with EV30 or EV71, the induction of mRNA synthesis for *IFNB*, *IFNL1* was severely impaired in P2's SV40-fibroblasts and in MDA5 KO SV40-fibroblasts relative to healthy control cells (Fig. 5, C and D). These results suggest that MDA5 is also an IFN-inducing sensor of both EV30 and EV71. In SV40-fibroblasts from P1 and a *TLR3*$^{-/-}$ HSE patient, similar or even stronger induction of *IFNB* and *IFNL1* than that in healthy control cells was observed upon infection with EV30 or EV71 (Fig. 5, C and D). Similar results were obtained in MDA5- and TLR3-deficient SV40-fibroblasts, in terms of induction of downstream IFN-stimulated genes (ISGs) including *CXCL10*, *MX1*, *OAS1*, and *ISG15*, upon infection with EV30 or EV71 (Fig. S3, A and B). Levels of *IFNB*, *IFNL1*, and the ISGs tested remained low 24 h after infection in SV40-fibroblasts from P1 and the *TLR3*$^{-/-}$ HSE patient, probably due to the low basal levels of these IFNs and ISGs in TLR3-deficient cells, although we cannot exclude the possibility that TLR3 also directly or indirectly regulates EV-induced IFN production to some extent. Together, these results confirm the critical role of TLR3 (but not MDA5) in maintaining basal cellular levels of antiviral IFN-α/β or -λ immunity (Gao et al., 2021), while also suggesting that EV-induced IFN-α/β or -λ production is dependent on MDA5 (but not TLR3). TLR3 and MDA5 may thus not only spatially but also sequentially control anti-EV immunity in CNS cells, via the maintenance of basal or virus-induced antiviral IFN-α/β or -λ levels, respectively.

Enhanced EV replication in the patients' fibroblasts early or late in infection

We then investigated cellular susceptibility to EV by measuring the kinetics of viral replication in SV40-fibroblasts from patients and controls. These cells are a well-established surrogate cell type for investigating the cell-intrinsic antiviral immunity of patients with viral encephalitis (Gao et al., 2021; Guo et al., 2011; Lim et al., 2019; Zhang et al., 2007). TLR3-deficient human SV40-fibroblasts are susceptible to various viruses, including HSV-1, VSV, IAV, and SARS-CoV-2, and MDA5-deficient human primary fibroblasts have independently been shown to be susceptible to rhinovirus (Asgari et al., 2017; Guo et al., 2011; Lamborn et al., 2017; Lim et al., 2019; Lim et al., 2014; Zhang et al., 2020; Zhang et al., 2007). We hypothesized that deficiencies of TLR3- or MDA5-dependent basal or virus-induced IFN-mediated immunity in cells would impair the control of EV infection and replication. We assessed the growth of EV30 (multiplicity of infection [MOI] 0.1) and EV71 (MOI 0.1) in SV40-fibroblasts from three healthy controls, P1, P2, a *TLR3*$^{-/-}$ HSE patient, an *IFNAR1*$^{-/-}$ HSE patient, and MDA5 KO SV40-fibroblasts. The levels of EV30 and EV71 replication were higher in cells from P1 and in fibroblasts from both the *TLR3*$^{-/-}$ and *IFNAR1*$^{-/-}$ patients than in cells from healthy controls as early as 10 h after infection for EV30, and 24 h after infection for EV71 (Fig. 6, A–D). Interestingly, virus levels were also higher in P2's SV40-fibroblasts and MDA5 KO SV40-fibroblasts than in cells from healthy controls, but at later time points than for the TLR3-deficient cells tested: 24 h after infection for EV30, and

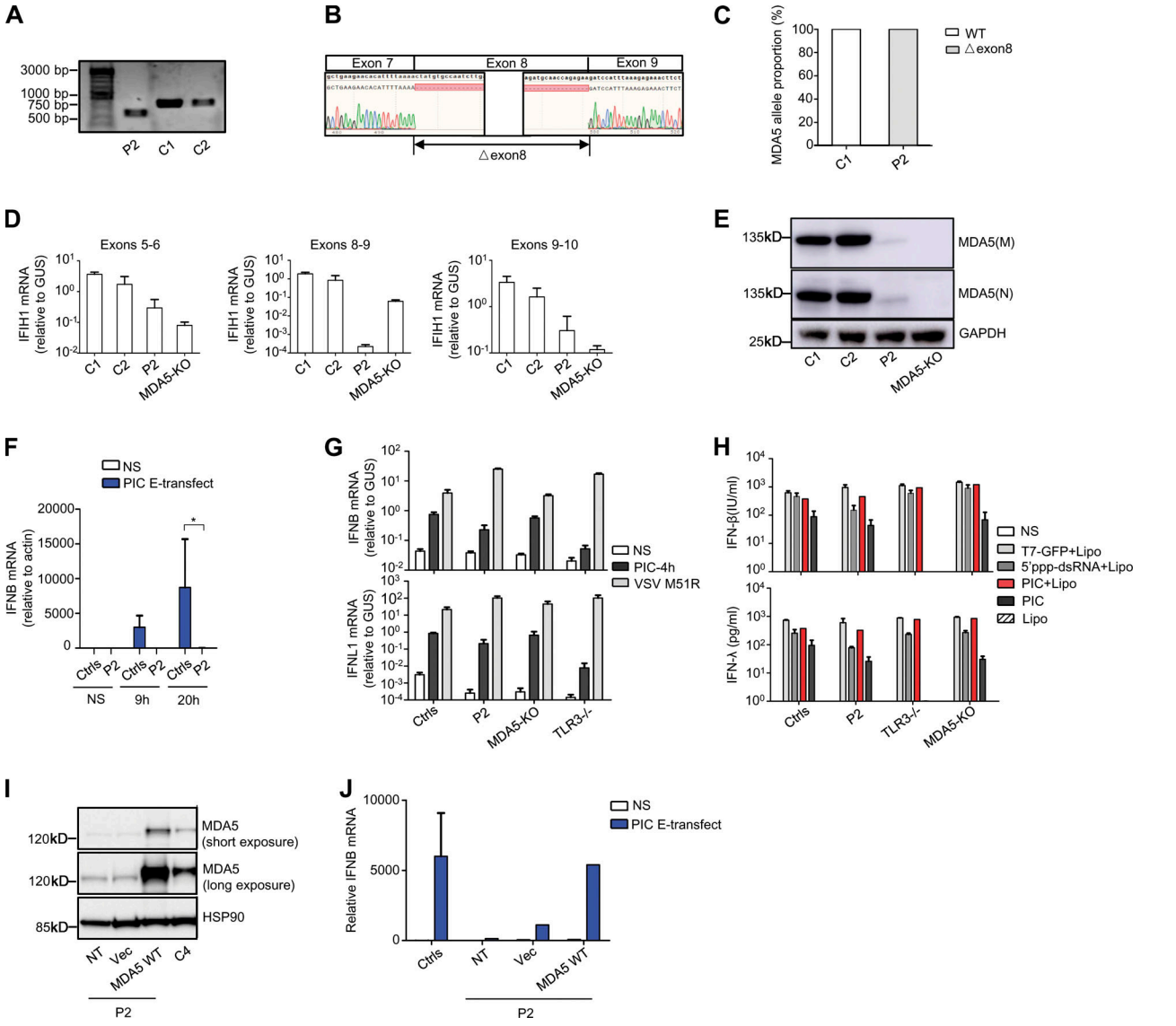

Figure 4. **Impairment of MDA5-dependent intracellular poly(I:C) responsiveness in P2's fibroblasts and rescue by WT MDA5. (A)** *IFIH1* PCR products from fibroblast cDNA, from P2 and two healthy controls (C1, C2), amplified with a forward primer binding to part of exon 6 and a reverse primer binding to part of exon 10. The result shown is representative of two independent experiments. **(B)** Sanger sequencing results for *IFIH1* from P2's fibroblast cDNA. **(C)** cDNA TOPO cloning and sequencing results demonstrating completely aberrant splicing of *IFIH1* in fibroblasts from P2. At least 50 transcripts were sequenced for the patient and the control. The result shown is the sum of two independent experiments. **(D)** *IFIH1* mRNA levels in SV40-fibroblasts from two healthy controls (C1, C2), P2, and MDA5 KO SV40-fibroblast, with primers spanning exons 5–6, exons 8–9, and exons 9–10, respectively; GUS was used as an expression control. Mean values and SD from three independent experiments, each with technical duplicates, are shown. **(E)** Western blot for MDA5 in SV40-fibroblasts from two healthy controls (C1, C2), P2, and MDA5 KO SV40-fibroblasts. One antibody recognizing aa 78–555 of MDA5 (M) and another recognizing the N-terminus of MDA5 (N) were used. GAPDH was used as a loading control. The data shown are representative of at least three independent experiments. **(F)** *IFNB* mRNA in primary fibroblasts from three healthy controls (Ctrls) and P2, without stimulation (NS), or after stimulation with intracellular poly(I:C) (PIC E-transfect: 10 ng/0.2 million cells, by nucleofection) for 9 and 20 h. P values were obtained by Student's *t* test by comparing P2's fibroblasts with all control fibroblasts after 20 h of stimulation with PIC E-transfect. *, $P < 0.05$. **(G)** *IFNB* and *IFNL1* mRNA levels in SV40-fibroblasts from three healthy controls (Ctrls), P2, MDA5 KO SV40-fibroblasts, or *TLR3*$^{-/-}$ patients, not stimulated (NS), stimulated for 4 h with extracellular 25 µg/ml poly(I:C), or infected with VSV M51R at an MOI of 1 for 18 h. GUS was included for normalization. Mean values and SD from three independent experiments are shown. **(H)** Production of IFN-β and IFN-λ in SV40-fibroblasts from two healthy controls (Ctrls), P2, MDA5 KO SV40-fibroblasts, or SV40-fibroblasts from a *TLR3*$^{-/-}$ patient, 24 h after stimulation with 0.2 µg/ml T7-GFP, 25 µg/ml 5'ppp-dsRNA, or 25 µg/ml poly(I:C), with or without Lipofectamine (Lipo), as assessed by ELISA. Mean values and SD from three independent experiments are shown. **(I)** MDA5 was detected by immunoblotting with an anti-MDA5 antibody, for SV40-fibroblast cells from one healthy control (C4), and from P2 without plasmid transfection (NT) or after transfection with the empty vector (Vec) or with WT *IFIH1*. **(J)** *IFNB* mRNA, in the absence of stimulation (NS), or after 6 h of stimulation with intracellular poly(I:C) (10 ng/0.2 million cells), as assessed by RT-qPCR, in SV40-fibroblasts from two healthy controls and P2, without plasmid transfection or after transfection with the empty vector (Vec) or with WT MDA5. Mean values ± SD were calculated from two controls tested in one experiment, representative of three independent experiments performed.

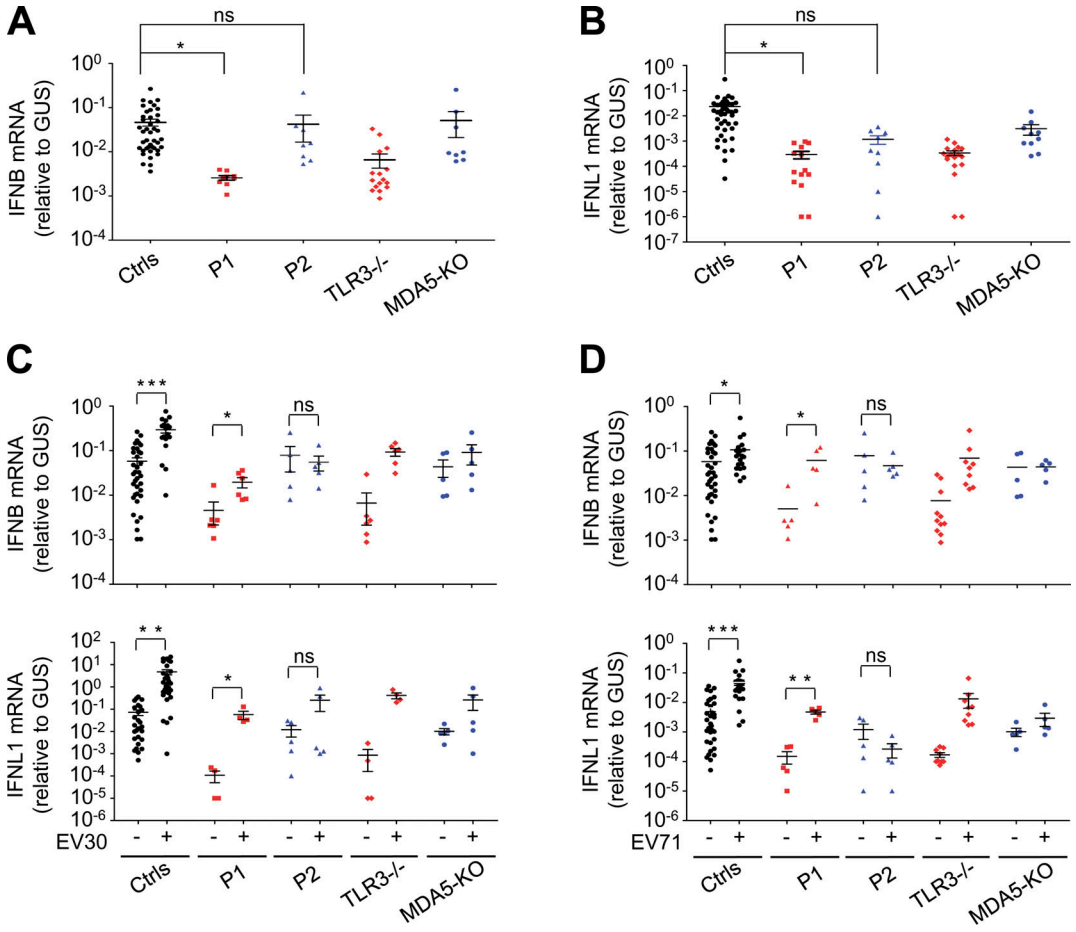

Figure 5. **Impaired basal or virus-induced IFN production in TLR3- or MDA5-deficient fibroblasts. (A and B)** mRNA levels for *IFNB* (A) and *IFNL1* (B) in unstimulated SV40-fibroblasts from three healthy controls (Ctrls), P1, P2, a *TLR3*$^{-/-}$ patient, and MDA5 KO SV40-fibroblasts, as quantified by RT-qPCR. **(C and D)** mRNA levels for *IFNB* and *IFNL1*, as assessed by RT-qPCR, in SV40-fibroblasts from three healthy controls (Ctrls), P1, P2, a *TLR3*$^{-/-}$ patient, and MDA5 KO SV40-fibroblasts, without viral infection, or following 24 h of infection with EV30 (C) or EV71 (D) at an MOI of 5. Data shown are from five independent experiments, with two biological replicates from each experiment (A and B), or three biological replicates from each experiment for the controls and one biological sample from each experiment for the patient-specific cell lines (C and D). Mean values ± SD were calculated from five independent experiments. P values were obtained by one-way ANOVA and subsequent least significant difference multiple comparison tests (A and B) or paired samples *t* test (C and D). ns, P > 0.05; *, P < 0.05; **, P < 0.01; ***, P < 0.001.

48 h after infection for EV71 (Fig. 6, A and B). Moreover, consistent with previous reports, high levels of viral replication and virus-induced cell death were observed for P1's SV40-fibroblasts following infection with HSV-1, similar to those observed for a *TLR3*$^{-/-}$ HSE patient and an *IFNAR1*$^{-/-}$ HSE patient, but higher than those for healthy control cells (Fig. S4, A and B). By contrast, P2's SV40-fibroblasts and MDA5 KO SV40-fibroblasts displayed normal resistance to HSV-1 at MOI 0.001 (Fig. S4, A and B). Finally, stable overexpression of exogeneous WT, but not D280N or F322fs2* TLR3, restored normal resistance to EV30 infection in P1's SV40-fibroblasts (Fig. 6 E), whereas stable overexpression of exogeneous WT MDA5 restored normal resistance to EV71 infection in SV40-fibroblasts from P2 (Fig. 6 F). Thus, TLR3, functioning as a "rheostat" of cell-intrinsic basal levels of antiviral immunity, appears to be crucial for the early control of a broad range of viruses, including EV, whereas MDA5 may be crucial for robust IFN induction upon infection with EV and other MDA5-dependent viruses. These results not only suggest that partial TLR3 deficiency and complete MDA5 deficiency underlie EVE in P1 and P2, respectively, but also suggest spatially and temporally different cellular mechanisms of disease.

IFN-α2b treatment rescued the EV replication phenotypes in TLR3- and MDA5-deficient fibroblasts in a time-dependent manner

We further assessed the different but cooperative roles of TLR3-dependent basal, and MDA5-dependent EV-induced, IFN-α/β and -λ antiviral immunity in the cellular control of EV infection, by studying the protective effect of IFN-α2b treatment against EV infection in human fibroblasts. As reported in previous studies (Gao et al., 2021; Lim et al., 2019), prior treatment with recombinant IFN-α2b, initiated 18 h before viral infection, boosted basal antiviral immunity and limited replication of the EV30 and EV71 viruses in SV40-fibroblasts from P1, P2, the *TLR3*$^{-/-}$ HSE patient, and MDA5 KO fibroblasts, but not in *IFNAR1*$^{-/-}$ fibroblasts (Hernandez et al., 2019; Fig. 6, A and B).

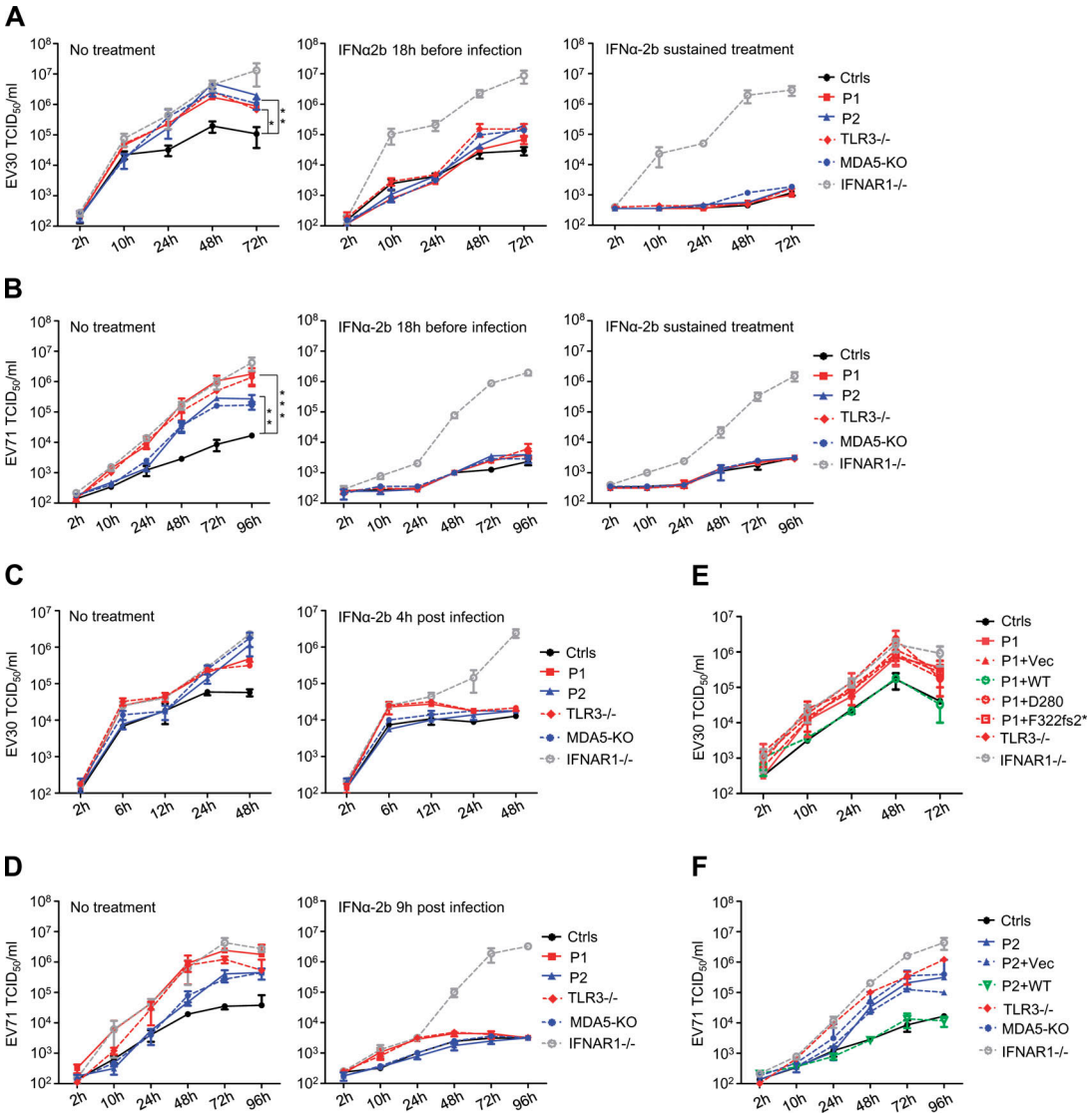

Figure 6. **Enhanced susceptibility to EV30 and EV71 in fibroblasts with TLR3 and MDA5 mutations, and rescue by WT TLR3 or MDA5 or by IFN-α2b treatment. (A–D)** Replication of EV30 (A and C) and EV71 (B and D), quantified by viral titration, in SV40-fibroblasts from three healthy controls (Ctrls), P1, P2, a *TLR3*$^{-/-}$ patient, MDA5 KO SV40-fibroblasts, and SV40-fibroblasts from an *IFNAR1*$^{-/-}$ patient, following infection with EV30 or EV71 at an MOI of 0.1, at various time points. IFN-α2b treatment was initiated 18 h before infection, then removed upon or continued during infection (A and B), or was started 4 h or 9 h after infection (C and D). **(E)** EV30 replication was assessed by viral titration, in SV40-fibroblasts from P1 that were left untransfected, or were transfected with an empty vector (Vec), *TLR3* WT, or *TLR3* D280N or F322fs2*, at various time points after infection, at an MOI of 0.1. **(F)** EV71 replication was evaluated by viral titration in SV40-fibroblasts from three healthy controls (Ctrls), or from P2 after stable transduction with WT MDA5 or empty vector (Vec), at various time points after infection at an MOI of 0.1. **(A–F)** Mean values ± SD from at least two independent experiments are shown. P values were obtained through log transformation followed by one-way ANOVA and subsequent Tukey's multiple comparison tests (A and B). *, P < 0.05; **, P < 0.01; ***, P < 0.001.

In other experiments, IFN-α2b treatment was started 4 or 9 h after infection with EV30 or EV71, to mimic the effect of virus-induced IFN-α/β or -λ production, which became detectable at about these time points (Fig. S4 C). Under such conditions, the enhanced viral replication phenotype was completely rescued in P2's SV40-fibroblasts and in MDA5 KO SV40-fibroblasts, but was only partially rescued in the SV40-fibroblasts of P1 and the *TLR3*$^{-/-}$ patient (Fig. 6, C and D). Finally, sustained IFN-α2b treatment, beginning 18 h before viral infection and continuing throughout infection, completely protected TLR3- or MDA5-deficient fibroblasts against the replication of EV30 and EV71 (Fig. 6, A and B). These data therefore provide further evidence that cellular TLR3-dependent basal IFN-α/β levels, and MDA5-dependent EV-induced, IFN-α/β antiviral immunity, are each essential for the cellular control of EV infection, either as an immediate first-line defense mechanism (TLR3) or later, following activation by viral infection (MDA5).

Discussion

Since the first reports of patients with EVE in the 1950s (Frothingham, 1958; Lennette et al., 1959; McAllister et al., 1959), numerous studies have been conducted to improve our understanding of the neurovirulence of EV (Evans et al., 1985; Fujii

et al., 2018; Gromeier et al., 1996), or to develop EV vaccines (Wu et al., 2001; Yi et al., 2017), but the prevention and treatment of this condition remain a global public health challenge. This study provides proof-of-concept that EV rhombencephalitis in otherwise healthy children can be caused by single-gene inborn errors of immunity. The discovery of a partial form of AR TLR3 deficiency and a complete form of AR MDA5 deficiency as genetic etiologies of life-threatening EVE in children adds more weight to the emerging paradigm that viral encephalitis can be the consequence of viral infection and genetic predisposition. As for other forms of encephalitis caused by different viruses, most of the patients who develop EV rhombencephalitis are otherwise healthy and have no history of other severe infectious diseases, viral or otherwise. It has become increasingly clear that non-hematopoietic, cell-intrinsic CNS-specific immunity is crucial for host defenses against viruses in the brain (Andersen et al., 2015; Bastard et al., 2021; Casrouge et al., 2006; Gao et al., 2021; Guo et al., 2011; Herman et al., 2012; Jouanguy et al., 2020; Lafaille et al., 2019; Lim et al., 2014; Ogunjimi et al., 2017; Pérez de Diego et al., 2010; Sancho-Shimizu et al., 2011; Zhang, 2020; Zhang and Casanova, 2015; Zhang et al., 2018; Zhang et al., 2007; Zhang et al., 2019; Zimmer et al., 2018). AR and AD TLR3 deficiencies have been shown to impair cell-intrinsic type I IFN–mediated antiviral immunity in human cortical neurons, resulting in HSV-1 encephalitis (Guo et al., 2011; Lim et al., 2014; Zhang et al., 2007). MDA5 deficiencies have not previously been associated with viral encephalitis in humans. Within the CNS, TLR3 is expressed by microglia, astrocytes, oligodendrocytes, and neurons (Bsibsi et al., 2002), whereas MDA5 is expressed mostly by microglia and astrocytes, but also by neurons (Chauhan et al., 2010; Peltier et al., 2010). It has been shown that, in human neural stem cell–derived neurons and some human neuronal cell lines at least, EV71 can induce the production of IFN-β, which protects against viral infection (Huang et al., 2019). We show here that impaired cell-intrinsic TLR3- or MDA5-dependent type I IFN production in human fibroblasts increases susceptibility to EV30 and EV71 infections. By inference, similar mechanisms may operate in CNS-resident cells expressing one or both of the dsRNA receptors. The finding of TLR3 and MDA5 deficiencies in 2 of the 15 patients with EVE studied suggests that cell-intrinsic type I IFN immunity plays an important role in host defense against EV infections of the CNS, although we cannot exclude the possibility of a role for type III IFNs. By extrapolation, early treatment with IFN-α or IFN-β may be beneficial in patients with EVE.

AR and AD TLR3 and MDA5 deficiencies have been previously shown to impair cell-intrinsic antiviral immunity, and thus to underlie HSE (TLR3) or viral pneumonia (TLR3, MDA5) in otherwise healthy children (Guo et al., 2011; Lamborn et al., 2017; Lim et al., 2019; Lim et al., 2014; Zhang et al., 2020; Zhang et al., 2007). All the reported TLR3- or MDA5-deficient individuals have each had isolated severe viral infections of the CNS or the lung, such as HSE, IAV pneumonia, SARS-CoV-2 pneumonia, rhinovirus pneumonia, or other severe respiratory viral infections (Asgari et al., 2017; Guo et al., 2011; Lamborn et al., 2017; Lim et al., 2019; Lim et al., 2014; Zhang et al., 2020; Zhang et al., 2007). None of the reported patients has developed both viral encephalitis and viral pneumonia, attesting to the incomplete clinical penetrance of both infections, as observed in patients with other deficiencies of type I IFN immunity (Andersen et al., 2015; Ciancanelli et al., 2015; Herman et al., 2012; Hernandez et al., 2019; Sancho-Shimizu et al., 2011). Indeed, unlike DBR1 deficiencies, which affect a molecule that is highly expressed specifically in the human brainstem and underlie brainstem viral encephalitis with complete penetrance (Zhang et al., 2018), deficiencies of type I IFN production or response pathways affect molecules broadly expressed throughout the human body, and may therefore result in susceptibility to various severe viral infections, albeit with incomplete penetrance (Itan et al., 2015). Type I IFN immunity is a general first-line antiviral defense mechanism that operates across various cells and organs of the human body. The disruption of any critical component of this circuit has been predicted to result in vulnerability to various kinds of viral infection under natural conditions. However, the clinical penetrance for each viral infection is incomplete, even for IFNAR1 deficiency (Bastard et al., 2021; Hernandez et al., 2019; Meyts and Casanova, 2021; Zhang et al., 2020). This incomplete penetrance may be accounted for by viral and/or human modifying factors, which remain to be studied. The patients with partial TLR3 or complete MDA5 deficiency reported here have remained healthy, other than their single episodes of EV rhombencephalitis, although the intrafamilial segregation of the mutations suggests full penetrance for the development of EVE in each family. The penetrance of viral diseases, including EVE, HSE, and severe viral pneumonia, in individuals with TLR3 or MDA deficiency in the general population is incomplete, but its level is currently unknown. These individuals need careful clinical follow-up for viral diseases known to be associated with TLR3 or MDA deficiency, and perhaps for other viral diseases that have been observed in patients with other deficiencies of type I IFN immunity (Bastard et al., 2020; Casanova and Abel, 2020, 2021; Zhang et al., 2020).

Unlike the previously studied severe viral diseases, each of which was found to be related to one type I IFN–inducing pathway, pleiotropic mutations of which can underlie different viral illnesses, the two genetic etiologies of isolated EVE described here affect either TLR3 or MDA5, which govern two spatially and temporally different IFN-α/β–inducing dsRNA-sensing pathways. TLR3 acts in the endosomal compartment, governing tonic type I IFNs, whereas MDA5 acts in the cytoplasm, governing responses to EV (Kang et al., 2002; Krishnan et al., 2007). Tlr3 KO and Mda5 KO mice are each susceptible to some viral infections, but resistant to others (Abe et al., 2012; Abston et al., 2012; Gitlin et al., 2006; Hardarson et al., 2007; Kato et al., 2006; McCartney et al., 2011; Negishi et al., 2008; Richer et al., 2009; Zhang et al., 2013), although it should be borne in mind that the viral load, virus strain, infection route, and cell lines used in the experimental infection models may have ultimately influenced the infection outcome. In our study, both patients developed rhombencephalitis after infection with an EV, but the clinical course of disease was more severe in P2 than in P1. Our data suggest that disruption of one of the two dsRNA sensors underlies EVE in P1 and P2 through different but related mechanisms, with an impairment of cellular basal antiviral

IFN immunity (TLR3) as previously described (Gao et al., 2021) in one patient, and an impairment of MDA5-dependent virus-induced IFN-α/β production (MDA5) in the other. At least in the cell type expressing both sensors that we tested, MDA5 and TLR3 induced type I IFN responses with different magnitudes and kinetics. The impairment of IFN production via a general (TLR3) or virus-specific (MDA5) mechanism impairs the control of virus replication early or late in EV infection, thereby underlying EVE. Other different but complementary molecular and cellular mechanisms may further interconnect TLR3 and MDA5 in anti-EV immunity in the CNS, and should be dissected in future investigations. Endosomal TLR3 may facilitate the internalization of viral agonist into the cytoplasmic compartment containing MDA5, boosting MDA5 activation (Slater et al., 2010). TLR3 and MDA5 may each also be critical in some but not all brain-resident or peripheral cells, for the cell type–specific control of EV infection. Our finding of a partial form of TLR3 deficiency and a complete form of MDA5 deficiency underlying EVE in two patients suggests that the two IFN-inducing dsRNA sensors are both essential for and cooperate in human CNS antiviral defense. Both sensors were also previously shown to play an essential role in human immunity to viruses in the respiratory tract. The clinical penetrance for CNS and respiratory viral infections is incomplete in individuals with TLR3 or MDA5 deficiency. Future studies will attempt to define both the range of viral infections in patients with TLR3 or MDA deficiency and the mechanisms underlying incomplete clinical penetrance.

Materials and methods

Patients

We have enrolled a cohort of 15 EVE patients (aged 7 mo to 4 yr 4 mo old; 9 males and 5 females) who originated from Europe, Africa, and America but all live in Spain, and developed encephalitis due to infection with EV71 or EV30. In this cohort, we have focused on the two patients described in this paper (P1 and P2). P1 was born to nonconsanguineous parents of African ancestry living in Spain. There was no family history of unusual susceptibility to infectious diseases. P1 was healthy, with normal development, until the age of 3.5 yr, when he developed EV30 rhombencephalitis. After supportive treatment, he recovered well without sequelae. P2 was born to nonconsanguineous Spanish parents. He was healthy until the age of 1 yr, when he developed EV71 rhombencephalitis. After treatment with intravenous immunoglobulin therapy (2 mg/kg), three methylprednisolone pulses (30 ng/kg then tapered), he recovered and was discharged from hospital with mild dysphagia and aphonia. Written informed consent was obtained in the country of residence of each patient, in accordance with local regulations and with institutional review board approval. Experiments were conducted in the United States and France, in accordance with local regulations and with the approval of the institutional review board of The Rockefeller University and the Institute National de la Santé et de la Recherche Médicale, respectively.

WES and Sanger sequencing

Genomic DNA was isolated by phenol-chloroform extraction from peripheral blood cells or primary fibroblasts from the patient. DNA (3 µg) was sheared with a Covaris S2 Ultrasonicator (Covaris). An adapter-ligated library was prepared with the TruSeq DNA Sample Prep Kit (Illumina). Exome capture was performed with the SureSelect Human All Exon 50 Mb kit (Agilent Technologies). Paired-end sequencing was performed on an Illumina HiSeq 2000 (Illumina), generating 100-base reads. The sequences were aligned with the human genome reference sequence (hg19 build), with the Burrows-Wheeler Aligner. Downstream processing was performed with the Genome Analysis Toolkit (GATK), SAMtools, and Picard Tools (http://picard.sourceforge.net). Substitution and indel calls were made with the GATK Unified Genotyper and GATK IndelGenotyperV2, respectively. All calls with a Phred-scaled single nucleotide polymorphism quality ≤20 and a read coverage ≤2 were filtered out. All variants were annotated with annotation software developed in-house. For the Sanger sequencing of *TLR3* and *IFIH1* variants, the exons of *TLR3* and *IFIH1* were amplified by PCR, purified by ultracentrifugation through Sephadex G-50 Superfine resin (Amersham-Pharmacia-Biotech), and sequenced with the Big Dye Terminator Cycle Sequencing Kit on an ABI Prism 3700 apparatus (Applied Biosystems).

TOPO-TA cloning

RNA extracted from SV40-fibroblasts was reverse-transcribed with the SuperScript III First-Strand synthesis system for RT-PCR kit (18080–051), following the manufacturer's protocol, with random hexamers. The TOPO-TA cloning kit for sequencing (450030; Invitrogen) was then used for subsequent cloning. The products were used to transduce stellar competent cells. At least 100 colonies per subject were picked for P1, P2, and a healthy control. Finally, we performed PCR on these colonies and sequenced them with the primers *TLR3*-exon3-forward: 5′-CCAGGGTGTTTTCACGCAAT-3′; *TLR3*-exon4-reverse: 5′-AGC ATCAGTCGTTGAAGGCT-3′; *IFIH1*-exon6-forward: 5′-TTCCGC AAGGAGTTCCAACC-3′; and *IFIH1*-exon10-reverse: 5′-GGGCCT CATTGTACTTCCTCA-3′.

Cell culture

Primary cultures of human fibroblasts were established from skin biopsy specimens from patients or healthy controls. They were transformed with an SV40 vector, as previously described (Zhang et al., 2007), to create immortalized SV40-fibroblast cell lines. Stably transfected SV40-fibroblasts were obtained by transfecting cells with pTRIP-TLR3iresRFP or mutants (generated by mutagenesis with a kit from Invitrogen), using the Nucleofector X-001 program (Lonza), according to the manufacturer's protocol, with selection on puromycin (2 µg/ml). The TLR3-deficient P2.1 fibrosarcoma cell line was provided by D.W. Leaman (University of Toledo, Toledo, OH; Sun and Leaman, 2004). Stably transfected P2.1 cells were established by transfection with pUNO-TLR3 WT (Invivogen) or mutant constructs in the same vector, in the presence of Lipofectamine 2000, with selection on blasticidin (10 µg/ml). SV40-fibroblasts, P2.1, and Vero cells (American Type Culture Collection [ATCC]) were maintained in DMEM supplemented with 10% FCS.

Cell stimulation

SV40-fibroblasts were used to coat a 24-well plate at a density of 9×10^4 cells per well. The cells were stimulated 24 h later with the TLR3 agonist poly(I:C) (Amersham) at concentrations of 1, 5, and 25 µg/ml. Cells were also stimulated with 25 µg/ml poly(I:C), 0.2 µg/ml T7-GFP RNA, or 25 µg/ml 5′ppp-dsRNA in the presence of Lipofectamine 2000 (Invitrogen), according to the manufacturer's instructions. Cells or supernatants were harvested, and their cytokine mRNA and protein levels were assessed by RT-qPCR and ELISA, respectively. For the assessment of IFN production upon viral infection, we used EV30 (strain Bastianni; ATCC) and EV71 (strain H; ATCC), at an MOI of 5. After 24 h, cells and supernatants were collected for cytokine determinations by ELISA, and the measurement of RNA levels for IFN genes by RT-qPCR. We assessed the cellular response to MDA5-specific intracellular poly(I:C) stimulation by resuspending 0.2 million primary or SV40-fibroblasts in 20 µl P3 nucleofection solution with 10 ng poly(I:C), and subjecting them to nucleofection with a 4D nucleofector system and the DT-130 program.

RT-qPCR

Total RNA was extracted from SV40-fibroblasts or P2.1 cells with the RNeasy mini kit (QIAGEN). The extracted RNA was treated with DNase I for 15 min at room temperature (QIAGEN). RNA was reverse-transcribed with random hexamers and the Superscript III first-strand cDNA synthesis system (Life Technologies). RT-qPCR was performed with the Taqman universal PCR master mix and Taqman gene expression kits from Life Technologies, using Taqman probes for *TLR3* (Hs01551079_g1 covering exons 4–5), *IFIH1* (Hs01070329_m1 covering exons 5–6; Hs01070332_m1 covering exons 8–9; Hs01070333_g1 covering exons 9–10), *CXCL10* (Hs00171042_m1 covering exons 1–2), *MX1* (Hs00895608_m1 covering exons 11–12), *OAS1* (Hs00973635_m1 covering exons 1–2), and *ISG15* (Hs00192713_m1 covering exons 1–2) with an ABI PRISM 7700 Sequence Detection System. We used β-glucuronidase (GUS) for normalization. Results were analyzed by the ΔCt method, in accordance with the kit manufacturer's instructions.

Cytokine determinations

Levels of IFN-β and -λ and IL-6 production were assessed by ELISA after 24 h of cell stimulation. Separate ELISAs were performed for IFN-β (PBL), IFN-λ (R&D Biosystems), and IL-6 (eBioscience) according to the kit manufacturers' instructions.

Immunoblots

Total cell extracts were prepared from SV40-fibroblasts and P2.1 cells. Cells were lysed in NP-40 lysis buffer (280 mM NaCl, 50 mM Tris, pH 8, 0.2 mM EDTA, 2 mM EGTA, 10% glycerol, and 0.5% NP-40) supplemented with 1 mM dithiothreitol, 1 mM Na_3VO_4, and Complete protease inhibitor cocktail (Roche). Equal amounts of protein from each sample were subjected to SDS-PAGE, and the proteins were blotted onto polyvinylidene difluoride membranes (Bio-Rad). The polyvinylidene difluoride membranes were then probed with an antibody against human TLR3 (R&D Systems) and an antibody against human MDA5 (Enzo Life Science and Cell Signaling Technology). Membranes were stripped and reprobed with an antibody against GAPDH (Sigma-Aldrich) or β-actin (Cell Signaling Technology) to control for protein loading. Antibody binding was detected by enhanced chemiluminescence (Amersham-Pharmacia-Biotech).

EV and HSV-1 infection and titration

For infection with viruses, 5×10^4 SV40-fibroblasts were plated in 48-well plates 1 d before infection. We used EV30 and EV71 at a MOI of 0.1 and HSV-1 at a MOI of 0.001 to infect cells in 500 µl DMEM supplemented with 10% FBS. After 2 h, the cells were washed once with Dulbecco's PBS and transferred to 500 µl DMEM supplemented with 2% FBS, in which they were maintained until harvesting at the various time points indicated. Where indicated, cells were treated with IFN-α2b (Intron A; Schering-Plough) at a concentration of 10^4 IU/ml before or after infection at various time points. Viral replication was assessed by determining viral titers on Vero cells, according to the Reed and Muench calculation (Zhang et al., 2007).

Cell viability assay

The viability of SV40-fibroblasts was assessed with a resazurin-based in vitro toxicology assay kit (Sigma-Aldrich). Cells were plated in triplicate in 96-well flat-bottomed plates (1.5×10^4 cells/well) in DMEM supplemented with 2% FBS. 24 h later, cells were infected with HSV-1 (strain KOS) at an MOI of 0.001. Resazurin dye was added to each well 48, 72, and 96 h later in an amount equivalent to 10% of the culture medium volume, and the plate was incubated for an additional 2 h in an incubator at 37°C. Absorbance at 600 nm was measured with a microplate reader, with the absorbance of uninfected cells considered to correspond to 100% viability.

Statistical analysis

When applicable, results are presented as mean ± SD. Mean values were compared between control cells and cells from the patients by a one-way ANOVA multiple comparison test or two-tailed Student's *t* test or paired samples *t* test. When indicated, linear mixed models were used for log-transformed relative values to account for repeated measurements. Statistical analysis was performed in SPSS 19.0. Statistical significance was denoted with ns, $P > 0.05$; *, $P < 0.05$; **, $P < 0.01$; and ***, $P < 0.001$ in the corresponding figures.

Online supplemental material

Fig. S1 shows biallelic *TLR3* or *IFIH1* mutations in two patients with EVE. Fig. S2 shows the function of P1's TLR3 mutants in vitro. Fig. S3 shows ISG induction in TLR3- or MDA5-deficient fibroblasts following EV30 or EV71 infection. Fig. S4 shows measurement of HSV-1 susceptibility and EV-induced IFN production in human SV40-fibroblasts. Table S1 shows homozygous and compound heterozygous rare nonsynonymous variants in P1. Table S2 shows homozygous and compound heterozygous rare nonsynonymous variants in P2.

Acknowledgments

We thank our patients and their families for participating in this study. We thank the members of both branches of the

Laboratory of Human Genetics of Infectious Diseases for helpful discussions; Tatiana Kochetkov for technical assistance; and Yelena Nemirovskaya for administrative assistance.

This work was funded in part by the National Center for Advancing Translational Sciences/National Institutes of Health/Clinical and Translational Science Award program (grant UL1TR001866); grants from the Agence Nationale de la Recherche under the "Investments for the Future" program (ANR-10-IAHU-01); Agence Nationale de la Recherche grants SEAeHostFactors (ANR-18-CE15-0020-02), GENVIR (ANR-20-CE93-003), and CNSVIRGEN (ANR-19-CE15-0009-01); the Rockefeller University; Institut National de la Santé et de la Recherche Médicale; University of Paris; and the St. Giles Foundation; and in part by the Division of Intramural Research, National Institute of Allergy and Infectious Diseases, National Institutes of Health.

Author contributions: J. Chen, H. Jing, W. Tung, and P. Bastard performed the experiments. J. Chen, H. Jing, A. Martin-Nalda, J.G. Rivière, R. Colobran, J. Manry, S. Boucherit, and M. Aubart analyzed the data. A. Martin-Nalda, J.G. Rivière, P. Soler Palacin, and R. Colobran recruited and treated the patients. M. Hasek, L. Lorenzo, Z. Liu, D. Lee, and F. Rozenberg helped in the design of the study and performed some of the experiments. L. Abel and H.C. Su contributed to the design of the study and data analysis. J.-L. Casanova and S-Y. Zhang conceptualized and supervised the project. J. Chen, J.-L. Casanova, and S-Y. Zhang wrote the manuscript. All authors contributed to and edited the manuscript.

Disclosures: The authors declare no competing interests exist.

Submitted: 22 June 2021
Revised: 31 August 2021
Accepted: 11 October 2021

References

Abe, Y., K. Fujii, N. Nagata, O. Takeuchi, S. Akira, H. Oshiumi, M. Matsumoto, T. Seya, and S. Koike. 2012. The toll-like receptor 3-mediated antiviral response is important for protection against poliovirus infection in poliovirus receptor transgenic mice. *J. Virol.* 86:185–194. https://doi.org/10.1128/JVI.05245-11

Abston, E.D., M.J. Coronado, A. Bucek, D. Bedja, J. Shin, J.B. Kim, E. Kim, K.L. Gabrielson, D. Georgakopoulos, W. Mitzner, and D. Fairweather. 2012. Th2 regulation of viral myocarditis in mice: different roles for TLR3 versus TRIF in progression to chronic disease. *Clin. Dev. Immunol.* 2012: 129486. https://doi.org/10.1155/2012/129486

Abzug, M.J., G. Cloud, J. Bradley, P.J. Sánchez, J. Romero, D. Powell, M. Lepow, C. Mani, E.V. Capparelli, S. Blount, et al. National Institute of Allergy and Infectious Diseases Collaborative Antiviral Study Group. 2003. Double blind placebo-controlled trial of pleconaril in infants with enterovirus meningitis. *Pediatr. Infect. Dis. J.* 22:335–341. https://doi.org/10.1097/01.inf.0000059765.92623.70

Alexopoulou, L., A.C. Holt, R. Medzhitov, and R.A. Flavell. 2001. Recognition of double-stranded RNA and activation of NF-kappaB by Toll-like receptor 3. *Nature.* 413:732–738. https://doi.org/10.1038/35099560

Andersen, L.L., N. Mørk, L.S. Reinert, E. Kofod-Olsen, R. Narita, S.E. Jørgensen, K.A. Skipper, K. Höning, H.H. Gad, L. Østergaard, et al. 2015. Functional IRF3 deficiency in a patient with herpes simplex encephalitis. *J. Exp. Med.* 212:1371–1379. https://doi.org/10.1084/jem.20142274

Andrés, C., J. Vila, L. Gimferrer, M. Piñana, J. Esperalba, M.G. Codina, M. Barnés, M.C. Martín, F. Fuentes, S. Rubio, et al. 2019. Surveillance of enteroviruses from paediatric patients attended at a tertiary hospital in Catalonia from 2014 to 2017. *J. Clin. Virol.* 110:29–35. https://doi.org/10.1016/j.jcv.2018.11.004

Antona, D., M. Kossorotoff, I. Schuffenecker, A. Mirand, M. Leruez-Ville, C. Bassi, M. Aubart, F. Moulin, D. Lévy-Bruhl, C. Henquell, et al. 2016. Severe paediatric conditions linked with EV-A71 and EV-D68, France, May to October 2016. *Euro Surveill.* 21:30402. https://doi.org/10.2807/1560-7917.ES.2016.21.46.30402

Asgari, S., L.J. Schlapbach, S. Anchisi, C. Hammer, I. Bartha, T. Junier, G. Mottet-Osman, K.M. Posfay-Barbe, D. Longchamp, M. Stocker, et al. 2017. Severe viral respiratory infections in children with *IFIH1* loss-of-function mutations. *Proc. Natl. Acad. Sci. USA.* 114:8342–8347. https://doi.org/10.1073/pnas.1704259114

Aubart, M., C. Gitiaux, C.J. Roux, R. Levy, I. Schuffenecker, A. Mirand, N. Bach, F. Moulin, J. Bergounioux, M. Leruez-Ville, et al. 2020. Severe Acute Flaccid Myelitis Associated With Enterovirus in Children: Two Phenotypes for Two Evolution Profiles? *Front. Neurol.* 11:343. https://doi.org/10.3389/fneur.2020.00343

Bastard, P., L.B. Rosen, Q. Zhang, E. Michailidis, H.H. Hoffmann, Y. Zhang, K. Dorgham, Q. Philippot, J. Rosain, V. Béziat, et al. COVID Human Genetic Effort. 2020. Autoantibodies against type I IFNs in patients with life-threatening COVID-19. *Science.* 370:eabd4585. https://doi.org/10.1126/science.abd4585

Bastard, P., J. Manry, J. Chen, J. Rosain, Y. Seeleuthner, O. AbuZaitun, L. Lorenzo, T. Khan, M. Hasek, N. Hernandez, et al. 2021. Herpes simplex encephalitis in a patient with a distinctive form of inherited IFNAR1 deficiency. *J. Clin. Invest.* 131:e139980. https://doi.org/10.1172/JCI139980

Bearden, D., M. Collett, P.L. Quan, B.T. Costa-Carvalho, and K.E. Sullivan. 2016. Enteroviruses in X-Linked Agammaglobulinemia: Update on Epidemiology and Therapy. *J. Allergy Clin. Immunol. Pract.* 4:1059–1065. https://doi.org/10.1016/j.jaip.2015.12.015

Bsibsi, M., R. Ravid, D. Gveric, and J.M. van Noort. 2002. Broad expression of Toll-like receptors in the human central nervous system. *J. Neuropathol. Exp. Neurol.* 61:1013–1021. https://doi.org/10.1093/jnen/61.11.1013

Cabrerizo, M., J.E. Echevarria, I. González, T. de Miguel, and G. Trallero. 2008. Molecular epidemiological study of HEV-B enteroviruses involved in the increase in meningitis cases occurred in Spain during 2006. *J. Med. Virol.* 80:1018–1024. https://doi.org/10.1002/jmv.21197

Casanova, J.L., and L. Abel. 2020. The human genetic determinism of life-threatening infectious diseases: genetic heterogeneity and physiological homogeneity? *Hum. Genet.* 139:681–694. https://doi.org/10.1007/s00439-020-02184-w

Casanova, J.L., and L. Abel. 2021. Lethal Infectious Diseases as Inborn Errors of Immunity: Toward a Synthesis of the Germ and Genetic Theories. *Annu. Rev. Pathol.* 16:23–50. https://doi.org/10.1146/annurev-pathol-031920-101429

Casanova, J.L., M.E. Conley, S.J. Seligman, L. Abel, and L.D. Notarangelo. 2014. Guidelines for genetic studies in single patients: lessons from primary immunodeficiencies. *J. Exp. Med.* 211:2137–2149. https://doi.org/10.1084/jem.20140520

Casrouge, A., S.Y. Zhang, C. Eidenschenk, E. Jouanguy, A. Puel, K. Yang, A. Alcais, C. Picard, N. Mahfoufi, N. Nicolas, et al. 2006. Herpes simplex virus encephalitis in human UNC-93B deficiency. *Science.* 314:308–312. https://doi.org/10.1126/science.1128346

Chan, L.G., U.D. Parashar, M.S. Lye, F.G. Ong, S.R. Zaki, J.P. Alexander, K.K. Ho, L.L. Han, M.A. Pallansch, A.B. Suleiman, et al. Outbreak Study Group. 2000. Deaths of children during an outbreak of hand, foot, and mouth disease in sarawak, malaysia: clinical and pathological characteristics of the disease. *Clin. Infect. Dis.* 31:678–683. https://doi.org/10.1086/314032

Chang, L.Y., H.Y. Lin, S.S. Gau, C.Y. Lu, S.H. Hsia, Y.C. Huang, L.M. Huang, and T.Y. Lin. 2019. Enterovirus A71 neurologic complications and long-term sequelae. *J. Biomed. Sci.* 26:57. https://doi.org/10.1186/s12929-019-0552-7

Chauhan, V.S., S.R. Furr, D.G. Sterka Jr., D.A. Nelson, M. Moerdyk-Schauwecker, I. Marriott, and V.Z. Grdzelishvili. 2010. Vesicular stomatitis virus infects resident cells of the central nervous system and induces replication-dependent inflammatory responses. *Virology.* 400:187–196. https://doi.org/10.1016/j.virol.2010.01.025

Chen, C.S., Y.C. Yao, S.C. Lin, Y.P. Lee, Y.F. Wang, J.R. Wang, C.C. Liu, H.Y. Lei, and C.K. Yu. 2007. Retrograde axonal transport: a major transmission route of enterovirus 71 in mice. *J. Virol.* 81:8996–9003. https://doi.org/10.1128/JVI.00236-07

Chen, B.S., H.C. Lee, K.M. Lee, Y.N. Gong, and S.R. Shih. 2020. Enterovirus and Encephalitis. *Front. Microbiol.* 11:261. https://doi.org/10.3389/fmicb.2020.00261

Choe, J., M.S. Kelker, and I.A. Wilson. 2005. Crystal structure of human toll-like receptor 3 (TLR3) ectodomain. *Science.* 309:581–585. https://doi.org/10.1126/science.1115253

Ciancanelli, M.J., S.X. Huang, P. Luthra, H. Garner, Y. Itan, S. Volpi, F.G. Lafaille, C. Trouillet, M. Schmolke, R.A. Albrecht, et al. 2015. Infectious disease. Life-threatening influenza and impaired interferon amplification in human IRF7 deficiency. *Science.* 348:448–453. https://doi.org/10.1126/science.aaa1578

Dalwai, A., S. Ahmad, A. Pacsa, and W. Al-Nakib. 2009. Echovirus type 9 is an important cause of viral encephalitis among infants and young children in Kuwait. *J. Clin. Virol.* 44:48–51. https://doi.org/10.1016/j.jcv.2008.10.007

de Crom, S.C., J.W. Rossen, A.M. van Furth, and C.C. Obihara. 2016. Enterovirus and parechovirus infection in children: a brief overview. *Eur. J. Pediatr.* 175:1023–1029. https://doi.org/10.1007/s00431-016-2725-7

Dropulic, L.K., and J.I. Cohen. 2011. Severe viral infections and primary immunodeficiencies. *Clin. Infect. Dis.* 53:897–909. https://doi.org/10.1093/cid/cir610

Evans, D.M., G. Dunn, P.D. Minor, G.C. Schild, A.J. Cann, G. Stanway, J.W. Almond, K. Currey, and J.V. Maizel Jr. 1985. Increased neurovirulence associated with a single nucleotide change in a noncoding region of the Sabin type 3 poliovaccine genome. *Nature.* 314:548–550. https://doi.org/10.1038/314548a0

Fowlkes, A.L., S. Honarmand, C. Glaser, S. Yagi, D. Schnurr, M.S. Oberste, L. Anderson, M.A. Pallansch, and N. Khetsuriani. 2008. Enterovirus-associated encephalitis in the California encephalitis project, 1998-2005. *J. Infect. Dis.* 198:1685–1691. https://doi.org/10.1086/592988

Frothingham, T.E. 1958. ECHO virus type 9 associated with three cases simulating meningococcemia. *N. Engl. J. Med.* 259:484–485. https://doi.org/10.1056/NEJM195809042591007

Fujii, K., Y. Sudaka, A. Takashino, K. Kobayashi, C. Kataoka, T. Suzuki, N. Iwata-Yoshikawa, O. Kotani, Y. Ami, H. Shimizu, et al. 2018. VP1 Amino Acid Residue 145 of Enterovirus 71 Is a Key Residue for Its Receptor Attachment and Resistance to Neutralizing Antibody during Cynomolgus Monkey Infection. *J. Virol.* 92:e00682-18. https://doi.org/10.1128/JVI.00682-18

Gao, D., M.J. Ciancanelli, P. Zhang, O. Harschnitz, V. Bondet, M. Hasek, J. Chen, X. Mu, Y. Itan, A. Cobat, et al. 2021. TLR3 controls constitutive IFN-β antiviral immunity in human fibroblasts and cortical neurons. *J. Clin. Invest.* 131:e134529. https://doi.org/10.1172/JCI134529

Gitlin, L., W. Barchet, S. Gilfillan, M. Cella, B. Beutler, R.A. Flavell, M.S. Diamond, and M. Colonna. 2006. Essential role of mda-5 in type I IFN responses to polyriboinosinic:polyribocytidylic acid and encephalomyocarditis picornavirus. *Proc. Natl. Acad. Sci. USA.* 103:8459–8464. https://doi.org/10.1073/pnas.0603082103

Gromeier, M., L. Alexander, and E. Wimmer. 1996. Internal ribosomal entry site substitution eliminates neurovirulence in intergeneric poliovirus recombinants. *Proc. Natl. Acad. Sci. USA.* 93:2370–2375. https://doi.org/10.1073/pnas.93.6.2370

Guo, Y., M. Audry, M. Ciancanelli, L. Alsina, J. Azevedo, M. Herman, E. Anguiano, V. Sancho-Shimizu, L. Lorenzo, E. Pauwels, et al. 2011. Herpes simplex virus encephalitis in a patient with complete TLR3 deficiency: TLR3 is otherwise redundant in protective immunity. *J. Exp. Med.* 208:2083–2098. https://doi.org/10.1084/jem.20101568

Hardarson, H.S., J.S. Baker, Z. Yang, E. Purevjav, C.H. Huang, L. Alexopoulou, N. Li, R.A. Flavell, N.E. Bowles, and J.G. Vallejo. 2007. Toll-like receptor 3 is an essential component of the innate stress response in virus-induced cardiac injury. *Am. J. Physiol. Heart Circ. Physiol.* 292:H251–H258. https://doi.org/10.1152/ajpheart.00398.2006

Herman, M., M. Ciancanelli, Y.H. Ou, L. Lorenzo, M. Klaudel-Dreszler, E. Pauwels, V. Sancho-Shimizu, R. Pérez de Diego, A. Abhyankar, E. Israelsson, et al. 2012. Heterozygous TBK1 mutations impair TLR3 immunity and underlie herpes simplex encephalitis of childhood. *J. Exp. Med.* 209:1567–1582. https://doi.org/10.1084/jem.20111316

Hernandez, N., G. Bucciol, L. Moens, J. Le Pen, M. Shahrooei, E. Goudouris, A. Shirkani, M. Changi-Ashtiani, H. Rokni-Zadeh, E.H. Sayar, et al. 2019. Inherited IFNAR1 deficiency in otherwise healthy patients with adverse reaction to measles and yellow fever live vaccines. *J. Exp. Med.* 216:2057–2070. https://doi.org/10.1084/jem.20182295

Huang, C.C., C.C. Liu, Y.C. Chang, C.Y. Chen, S.T. Wang, and T.F. Yeh. 1999. Neurologic complications in children with enterovirus 71 infection. *N. Engl. J. Med.* 341:936–942. https://doi.org/10.1056/NEJM199909233411302

Huang, H.I., J.Y. Lin, and S.H. Chen. 2019. EV71 Infection Induces IFNβ Expression in Neural Cells. *Viruses.* 11:1121. https://doi.org/10.3390/v11121121

Itan, Y., L. Shang, B. Boisson, E. Patin, A. Bolze, M. Moncada-Vélez, E. Scott, M.J. Ciancanelli, F.G. Lafaille, J.G. Markle, et al. 2015. The human gene damage index as a gene-level approach to prioritizing exome variants. *Proc. Natl. Acad. Sci. USA.* 112:13615–13620. https://doi.org/10.1073/pnas.1518646112

Jones, T.P.W., M. Buckland, J. Breuer, and D.M. Lowe. 2019. Viral infection in primary antibody deficiency syndromes. *Rev. Med. Virol.* 29:e2049. https://doi.org/10.1002/rmv.2049

Jouanguy, E., V. Béziat, T.H. Mogensen, J.L. Casanova, S.G. Tangye, and S.Y. Zhang. 2020. Human inborn errors of immunity to herpes viruses. *Curr. Opin. Immunol.* 62:106–122. https://doi.org/10.1016/j.coi.2020.01.004

Jubelt, B., and H.L. Lipton. 2014. Enterovirus/picornavirus infections. *Handb. Clin. Neurol.* 123:379–416. https://doi.org/10.1016/B978-0-444-53488-0.00018-3

Kang, D.C., R.V. Gopalkrishnan, Q. Wu, E. Jankowsky, A.M. Pyle, and P.B. Fisher. 2002. mda-5: An interferon-inducible putative RNA helicase with double-stranded RNA-dependent ATPase activity and melanoma growth-suppressive properties. *Proc. Natl. Acad. Sci. USA.* 99:637–642. https://doi.org/10.1073/pnas.022637199

Kato, H., O. Takeuchi, S. Sato, M. Yoneyama, M. Yamamoto, K. Matsui, S. Uematsu, A. Jung, T. Kawai, K.J. Ishii, et al. 2006. Differential roles of MDA5 and RIG-I helicases in the recognition of RNA viruses. *Nature.* 441:101–105. https://doi.org/10.1038/nature04734

Krishnan, J., K. Selvarajoo, M. Tsuchiya, G. Lee, and S. Choi. 2007. Toll-like receptor signal transduction. *Exp. Mol. Med.* 39:421–438. https://doi.org/10.1038/emm.2007.47

Kumar, A., D. Shukla, R. Kumar, M.Z. Idris, U.K. Misra, and T.N. Dhole. 2011. An epidemic of encephalitis associated with human enterovirus B in Uttar Pradesh, India, 2008. *J. Clin. Virol.* 51:142–145. https://doi.org/10.1016/j.jcv.2011.02.011

Lafaille, F.G., O. Harschnitz, Y.S. Lee, P. Zhang, M.L. Hasek, G. Kerner, Y. Itan, O. Ewaleifoh, F. Rapaport, T.M. Carlile, et al. 2019. Human SNORA31 variations impair cortical neuron-intrinsic immunity to HSV-1 and underlie herpes simplex encephalitis. *Nat. Med.* 25:1873–1884. https://doi.org/10.1038/s41591-019-0672-3

Lamborn, I.T., H. Jing, Y. Zhang, S.B. Drutman, J.K. Abbott, S. Munir, S. Bade, H.M. Murdock, C.P. Santos, L.G. Brock, et al. 2017. Recurrent rhinovirus infections in a child with inherited MDA5 deficiency. *J. Exp. Med.* 214:1949–1972. https://doi.org/10.1084/jem.20161759

Lennette, E.H., R.L. Magoffin, N.J. Schmidt, and A.C. Hollister Jr. 1959. Viral disease of the central nervous system; influence of poliomyelitis vaccination on etiology. *J. Am. Med. Assoc.* 171:1456–1464. https://doi.org/10.1001/jama.1959.03010290014006

Lévêque, N., J. Jacques, F. Renois, D. Antona, M. Abely, J.J. Chomel, and L. Andréoletti. 2010. Phylogenetic analysis of Echovirus 30 isolated during the 2005 outbreak in France reveals existence of multiple lineages and suggests frequent recombination events. *J. Clin. Virol.* 48:137–141. https://doi.org/10.1016/j.jcv.2010.03.011

Lewthwaite, P., D. Perera, M.H. Ooi, A. Last, R. Kumar, A. Desai, A. Begum, V. Ravi, M.V. Shankar, P.H. Tio, et al. 2010. Enterovirus 75 encephalitis in children, southern India. *Emerg. Infect. Dis.* 16:1780–1782. https://doi.org/10.3201/eid1611.100672

Li, X., C. Lu, M. Stewart, H. Xu, R.K. Strong, T. Igumenova, and P. Li. 2009. Structural basis of double-stranded RNA recognition by the RIG-I like receptor MDA5. *Arch. Biochem. Biophys.* 488:23–33. https://doi.org/10.1016/j.abb.2009.06.008

Lim, H.K., M. Seppänen, T. Hautala, M.J. Ciancanelli, Y. Itan, F.G. Lafaille, W. Dell, L. Lorenzo, M. Byun, E. Pauwels, et al. 2014. TLR3 deficiency in herpes simplex encephalitis: high allelic heterogeneity and recurrence risk. *Neurology.* 83:1888–1897. https://doi.org/10.1212/WNL.0000000000000999

Lim, H.K., S.X.L. Huang, J. Chen, G. Kerner, O. Gilliaux, P. Bastard, K. Dobbs, N. Hernandez, N. Goudin, M.L. Hasek, et al. 2019. Severe influenza pneumonitis in children with inherited TLR3 deficiency. *J. Exp. Med.* 216:2038–2056. https://doi.org/10.1084/jem.20181621

Lin, T.Y., L.Y. Chang, S.H. Hsia, Y.C. Huang, C.H. Chiu, C. Hsueh, S.R. Shih, C.C. Liu, and M.H. Wu. 2002. The 1998 enterovirus 71 outbreak in Taiwan: pathogenesis and management. *Clin. Infect. Dis.* 34(Suppl 2):S52–S57. https://doi.org/10.1086/338819

Lin, T.Y., S.J. Twu, M.S. Ho, L.Y. Chang, and C.Y. Lee. 2003. Enterovirus 71 outbreaks, Taiwan: occurrence and recognition. *Emerg. Infect. Dis.* 9:291–293. https://doi.org/10.3201/eid0903.020285

McAllister, R.M., K. Hummeler, and L.L. Coriell. 1959. Acute Cerebellar Ataxia. *N. Engl. J. Med.* 261:1159–1162. https://doi.org/10.1056/NEJM195912032612304

McCartney, S.A., W. Vermi, S. Lonardi, C. Rossini, K. Otero, B. Calderon, S. Gilfillan, M.S. Diamond, E.R. Unanue, and M. Colonna. 2011. RNA sensor-induced type I IFN prevents diabetes caused by a β cell-tropic virus in mice. *J. Clin. Invest.* 121:1497–1507. https://doi.org/10.1172/JCI44005

McMinn, P., I. Stratov, L. Nagarajan, and S. Davis. 2001. Neurological manifestations of enterovirus 71 infection in children during an outbreak of hand, foot, and mouth disease in Western Australia. *Clin. Infect. Dis.* 32:236–242. https://doi.org/10.1086/318454

Mehndiratta, M.M., P. Mehndiratta, and R. Pande. 2014. Poliomyelitis: historical facts, epidemiology, and current challenges in eradication. *Neurohospitalist.* 4:223–229. https://doi.org/10.1177/1941874414533352

Meijer, A., S. van der Sanden, B.E. Snijders, G. Jaramillo-Gutierrez, L. Bont, C.K. van der Ent, P. Overduin, S.L. Jenny, E. Jusic, H.G. van der Avoort, et al. 2012. Emergence and epidemic occurrence of enterovirus 68 respiratory infections in The Netherlands in 2010. *Virology.* 423:49–57. https://doi.org/10.1016/j.virol.2011.11.021

Meyts, I., and J.L. Casanova. 2021. Viral infections in humans and mice with genetic deficiencies of the type I IFN response pathway. *Eur. J. Immunol.* 51:1039–1061. https://doi.org/10.1002/eji.202048793

Mikami, T., H. Miyashita, S. Takatsuka, Y. Kuroki, and N. Matsushima. 2012. Molecular evolution of vertebrate Toll-like receptors: evolutionary rate difference between their leucine-rich repeats and their TIR domains. *Gene.* 503:235–243. https://doi.org/10.1016/j.gene.2012.04.007

Mirand, A., I. Schuffenecker, C. Henquell, G. Billaud, G. Jugie, D. Falcon, A. Mahul, C. Archimbaud, E. Terletskaia-Ladwig, S. Diedrich, et al. 2010. Phylogenetic evidence for a recent spread of two populations of human enterovirus 71 in European countries. *J. Gen. Virol.* 91:2263–2277. https://doi.org/10.1099/vir.0.021741-0

Moore, M. 1982. Centers for Disease Control. Enteroviral disease in the United States, 1970-1979. *J. Infect. Dis.* 146:103–108. https://doi.org/10.1093/infdis/146.1.103

Negishi, H., T. Osawa, K. Ogami, X. Ouyang, S. Sakaguchi, R. Koshiba, H. Yanai, Y. Seko, H. Shitara, K. Bishop, et al. 2008. A critical link between Toll-like receptor 3 and type II interferon signaling pathways in antiviral innate immunity. *Proc. Natl. Acad. Sci. USA.* 105:20446–20451. https://doi.org/10.1073/pnas.0810372105

Ogunjimi, B., S.Y. Zhang, K.B. Sørensen, K.A. Skipper, M. Carter-Timofte, G. Kerner, S. Luecke, T. Prabakaran, Y. Cai, J. Meester, et al. 2017. Inborn errors in RNA polymerase III underlie severe varicella zoster virus infections. *J. Clin. Invest.* 127:3543–3556. https://doi.org/10.1172/JCI92280

Ong, K.C., M. Badmanathan, S. Devi, K.L. Leong, M.J. Cardosa, and K.T. Wong. 2008. Pathologic characterization of a murine model of human enterovirus 71 encephalomyelitis. *J. Neuropathol. Exp. Neurol.* 67:532–542. https://doi.org/10.1097/NEN.0b013e31817713e7

Peltier, D.C., A. Simms, J.R. Farmer, and D.J. Miller. 2010. Human neuronal cells possess functional cytoplasmic and TLR-mediated innate immune pathways influenced by phosphatidylinositol-3 kinase signaling. *J. Immunol.* 184:7010–7021. https://doi.org/10.4049/jimmunol.0904133

Pérez de Diego, R., V. Sancho-Shimizu, L. Lorenzo, A. Puel, S. Plancoulaine, C. Picard, M. Herman, A. Cardon, A. Durandy, J. Bustamante, et al. 2010. Human TRAF3 adaptor molecule deficiency leads to impaired Toll-like receptor 3 response and susceptibility to herpes simplex encephalitis. *Immunity.* 33:400–411. https://doi.org/10.1016/j.immuni.2010.08.014

Reikine, S., J.B. Nguyen, and Y. Modis. 2014. Pattern Recognition and Signaling Mechanisms of RIG-I and MDA5. *Front. Immunol.* 5:342. https://doi.org/10.3389/fimmu.2014.00342

Richer, M.J., D.J. Lavallée, I. Shanina, and M.S. Horwitz. 2009. Toll-like receptor 3 signaling on macrophages is required for survival following coxsackievirus B4 infection. *PLoS One.* 4:e4127. https://doi.org/10.1371/journal.pone.0004127

Rudolph, H., R. Prieto Dernbach, M. Walka, P. Rey-Hinterkopf, V. Melichar, E. Muschiol, S. Schweitzer-Krantz, J.W. Richter, C. Weiss, S. Böttcher, et al. 2017. Comparison of clinical and laboratory characteristics during two major paediatric meningitis outbreaks of echovirus 30 and other non-polio enteroviruses in Germany in 2008 and 2013. *Eur. J. Clin. Microbiol. Infect. Dis.* 36:1651–1660. https://doi.org/10.1007/s10096-017-2979-7

Sancho-Shimizu, V., R. Pérez de Diego, L. Lorenzo, R. Halwani, A. Alangari, E. Israelsson, S. Fabrega, A. Cardon, J. Maluenda, M. Tatematsu, et al. 2011. Herpes simplex encephalitis in children with autosomal recessive and dominant TRIF deficiency. *J. Clin. Invest.* 121:4889–4902. https://doi.org/10.1172/JCI59259

Shih, S.R., M.S. Ho, K.H. Lin, S.L. Wu, Y.T. Chen, C.N. Wu, T.Y. Lin, L.Y. Chang, K.C. Tsao, H.C. Ning, et al. 2000. Genetic analysis of enterovirus 71 isolated from fatal and non-fatal cases of hand, foot and mouth disease during an epidemic in Taiwan, 1998. *Virus Res.* 68:127–136. https://doi.org/10.1016/S0168-1702(00)00162-3

Slade, C.A., C. McLean, T. Scerri, T.B. Giang, S. Megaloudis, A. Strathmore, J.C. Tempany, K. Nicholls, C. D'Arcy, M. Bahlo, et al. 2019. Fatal Enteroviral Encephalitis in a Patient with Common Variable Immunodeficiency Harbouring a Novel Mutation in NFKB2. *J. Clin. Immunol.* 39:324–335. https://doi.org/10.1007/s10875-019-00602-x

Slater, L., N.W. Bartlett, J.J. Haas, J. Zhu, S.D. Message, R.P. Walton, A. Sykes, S. Dahdaleh, D.L. Clarke, M.G. Belvisi, et al. 2010. Co-ordinated role of TLR3, RIG-I and MDA5 in the innate response to rhinovirus in bronchial epithelium. *PLoS Pathog.* 6:e1001178. https://doi.org/10.1371/journal.ppat.1001178

Sun, Y., and D.W. Leaman. 2004. Ectopic expression of toll-like receptor-3 (TLR-3) overcomes the double-stranded RNA (dsRNA) signaling defects of P2.1 cells. *J. Interferon Cytokine Res.* 24:350–361. https://doi.org/10.1089/107999004323142213

Tang, Y.W., P.J. Cleavinger, H. Li, P.S. Mitchell, T.F. Smith, and D.H. Persing. 2000. Analysis of candidate-host immunogenetic determinants in herpes simplex virus-associated Mollaret's meningitis. *Clin. Infect. Dis.* 30:176–178. https://doi.org/10.1086/313616

Thoa, P.K., P.S. Chiang, T.H. Khanh, S.T. Luo, T.N. Dan, Y.F. Wang, T.C. Thuong, W.Y. Chung, N.T. Hung, J.R. Wang, et al. 2013. Genetic and antigenic characterization of enterovirus 71 in Ho Chi Minh City, Vietnam, 2011. *PLoS One.* 8:e69895. https://doi.org/10.1371/journal.pone.0069895

Trallero, G., A. Avellon, A. Otero, T. De Miguel, C. Pérez, N. Rabella, G. Rubio, J.E. Echevarria, and M. Cabrerizo. 2010. Enteroviruses in Spain over the decade 1998-2007: virological and epidemiological studies. *J. Clin. Virol.* 47:170–176. https://doi.org/10.1016/j.jcv.2009.11.013

van der Linden, L., K.C. Wolthers, and F.J. van Kuppeveld. 2015. Replication and Inhibitors of Enteroviruses and Parechoviruses. *Viruses.* 7:4529–4562. https://doi.org/10.3390/v7082832

Wang, Q., D.R. Nagarkar, E.R. Bowman, D. Schneider, B. Gosangi, J. Lei, Y. Zhao, C.L. McHenry, R.V. Burgens, D.J. Miller, et al. 2009. Role of double-stranded RNA pattern recognition receptors in rhinovirus-induced airway epithelial cell responses. *J. Immunol.* 183:6989–6997. https://doi.org/10.4049/jimmunol.0901386

Winkelstein, J.A., M.C. Marino, H.M. Lederman, S.M. Jones, K. Sullivan, A.W. Burks, M.E. Conley, C. Cunningham-Rundles, and H.D. Ochs. 2006. X-linked agammaglobulinemia: report on a United States registry of 201 patients. *Medicine (Baltimore).* 85:193–202. https://doi.org/10.1097/01.md.0000229482.27398.ad

Wörner, N., R. Rodrigo-García, A. Antón, E. Castellarnau, I. Delgado, È. Vazquez, S. González, L. Mayol, M. Méndez, E. Solé, et al. 2021. Enterovirus-A71 Rhombencephalitis Outbreak in Catalonia: Characteristics, Management and Outcome. *Pediatr. Infect. Dis. J.* 40:628–633. https://doi.org/10.1097/INF.0000000000003114

Wu, B., and S. Hur. 2015. How RIG-I like receptors activate MAVS. *Curr. Opin. Virol.* 12:91–98. https://doi.org/10.1016/j.coviro.2015.04.004

Wu, C.N., Y.C. Lin, C. Fann, N.S. Liao, S.R. Shih, and M.S. Ho. 2001. Protection against lethal enterovirus 71 infection in newborn mice by passive immunization with subunit VP1 vaccines and inactivated virus. *Vaccine.* 20:895–904. https://doi.org/10.1016/S0264-410X(01)00385-1

Wu, Y., A. Yeo, M.C. Phoon, E.L. Tan, C.L. Poh, S.H. Quak, and V.T. Chow. 2010. The largest outbreak of hand; foot and mouth disease in Singapore in 2008: the role of enterovirus 71 and coxsackievirus A strains. *Int. J. Infect. Dis.* 14:e1076–e1081. https://doi.org/10.1016/j.ijid.2010.07.006

Xiang, Z., R. Gonzalez, Z. Wang, L. Ren, Y. Xiao, J. Li, Y. Li, G. Vernet, G. Paranhos-Baccalà, Q. Jin, and J. Wang. 2012. Coxsackievirus A21, enterovirus 68, and acute respiratory tract infection, China. *Emerg. Infect. Dis.* 18:821–824. https://doi.org/10.3201/eid1805.111376

Yang, W.X., T. Terasaki, K. Shiroki, S. Ohka, J. Aoki, S. Tanabe, T. Nomura, E. Terada, Y. Sugiyama, and A. Nomoto. 1997. Efficient delivery of circulating poliovirus to the central nervous system independently of poliovirus receptor. *Virology.* 229:421–428. https://doi.org/10.1006/viro.1997.8450

Yi, E.J., Y.J. Shin, J.H. Kim, T.G. Kim, and S.Y. Chang. 2017. Enterovirus 71 infection and vaccines. *Clin. Exp. Vaccine Res.* 6:4–14. https://doi.org/10.7774/cevr.2017.6.1.4

Zeng, M., N.F. El Khatib, S. Tu, P. Ren, S. Xu, Q. Zhu, X. Mo, D. Pu, X. Wang, and R. Altmeyer. 2012. Seroepidemiology of Enterovirus 71 infection prior to the 2011 season in children in Shanghai. *J. Clin. Virol.* 53:285–289. https://doi.org/10.1016/j.jcv.2011.12.025

Zhang, S.Y. 2020. Herpes simplex virus encephalitis of childhood: inborn errors of central nervous system cell-intrinsic immunity. *Hum. Genet.* 139:911–918. https://doi.org/10.1007/s00439-020-02127-5

Zhang, S.Y., and J.L. Casanova. 2015. Inborn errors underlying herpes simplex encephalitis: From TLR3 to IRF3. *J. Exp. Med.* 212:1342–1343. https://doi.org/10.1084/jem.2129insight4

Zhang, S.Y., E. Jouanguy, S. Ugolini, A. Smahi, G. Elain, P. Romero, D. Segal, V. Sancho-Shimizu, L. Lorenzo, A. Puel, et al. 2007. TLR3 deficiency in patients with herpes simplex encephalitis. *Science.* 317:1522–1527. https://doi.org/10.1126/science.1139522

Zhang, S.Y., M. Herman, M.J. Ciancanelli, R. Pérez de Diego, V. Sancho-Shimizu, L. Abel, and J.L. Casanova. 2013. TLR3 immunity to infection in mice and humans. *Curr. Opin. Immunol.* 25:19–33. https://doi.org/10.1016/j.coi.2012.11.001

Zhang, S.Y., N.E. Clark, C.A. Freije, E. Pauwels, A.J. Taggart, S. Okada, H. Mandel, P. Garcia, M.J. Ciancanelli, A. Biran, et al. 2018. Inborn Errors of RNA Lariat Metabolism in Humans with Brainstem Viral Infection. *Cell.* 172:952–965.e18. https://doi.org/10.1016/j.cell.2018.02.019

Zhang, S.Y., E. Jouanguy, Q. Zhang, L. Abel, A. Puel, and J.L. Casanova. 2019. Human inborn errors of immunity to infection affecting cells other than leukocytes: from the immune system to the whole organism. *Curr. Opin. Immunol.* 59:88–100. https://doi.org/10.1016/j.coi.2019.03.008

Zhang, Q., P. Bastard, Z. Liu, J. Le Pen, M. Moncada-Velez, J. Chen, M. Ogishi, I.K.D. Sabli, S. Hodeib, C. Korol, et al. NIAID-USUHS/TAGC COVID Immunity Group. 2020. Inborn errors of type I IFN immunity in patients with life-threatening COVID-19. *Science.* 370:eabd4570. https://doi.org/10.1126/science.abd4570

Zimmer, B., O. Ewaleifoh, O. Harschnitz, Y.S. Lee, C. Peneau, J.L. McAlpine, B. Liu, J. Tchieu, J.A. Steinbeck, F. Lafaille, et al. 2018. Human iPSC-derived trigeminal neurons lack constitutive TLR3-dependent immunity that protects cortical neurons from HSV-1 infection. *Proc. Natl. Acad. Sci. USA.* 115:E8775–E8782. https://doi.org/10.1073/pnas.1809853115

Supplemental material

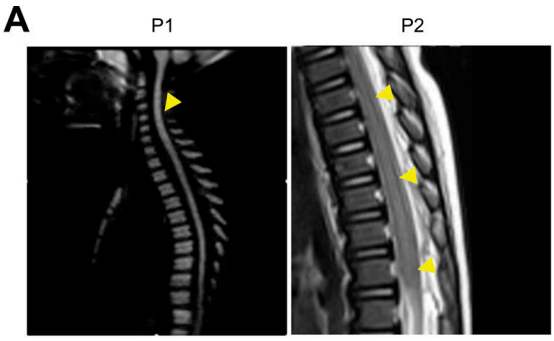

B

	HSV-1	HSV-2	IAV	IBV	RSV	Para influenza III	Measles	Mumps	Rubella
P1	16.7	N	N	N	N	256	>300	266	39
P2	16.7	N	NA	NA	NA	NA	165	50	65
Threshold	1.1	1.1	4	4	4	4	11	10	20

Note: IAV Influenza A Virus; IBV Influenza B Virus; RSV Respiratory Syncytial Virus

C

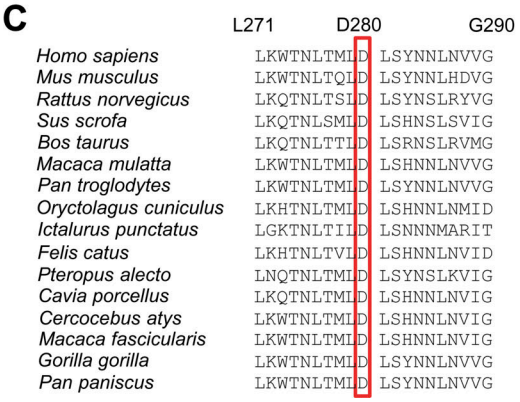

Figure S1. **Biallelic *TLR3* or *IFIH1* mutations in two patients with EVE. (A)** Brain imaging showing EVE lesions in P1 and P2. In P1, post-contrast T1-FLAIR imaging showed pathological tegmental hypersignal (yellow arrows) associated with cervical myelitis, highly suggestive of rhombencephalitis. In P2, post-contrast T1-FLAIR imaging showed pathological tegmental hypersignal, with evidence of diffusion restriction in the superior cerebellar peduncles and the ponto-bulbar junction (yellow arrows), suggestive of rhombencephalitis. **(B)** Tests for IgG antibodies against various viruses were performed at the age of 8 yr for P1, and at the age of 5 yr for P2. The threshold value for each viral serological test is indicated. N, negative; NA, not applicable. **(C)** Alignment of TLR3 protein sequences around the D280 residue, across species.

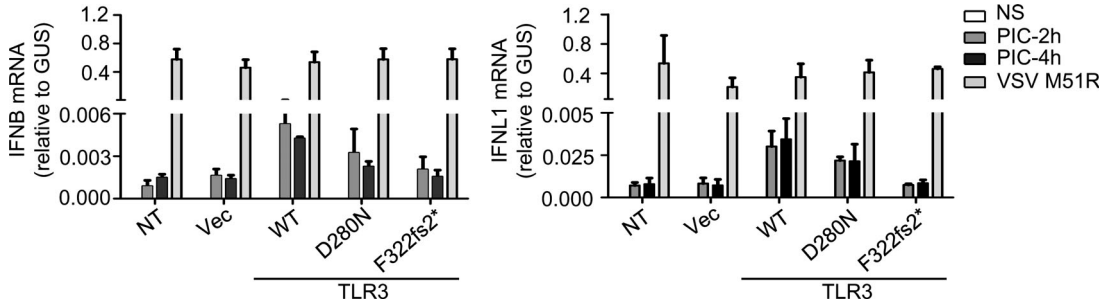

Figure S2. **Function of P1's TLR3 mutants in vitro.** RT-qPCR for *IFNB* and *IFNL1* mRNA levels, without stimulation (NS) or after 2 and 4 h of stimulation with 25 µg/ml poly(I:C) (PIC), in P2.1 cells not transfected (NT) or stably transfected with empty vector (Vec), HA-tagged *TLR3* WT, D280N, or F322fs2*. VSV M51R, at an MOI of 1, was used as a positive control for IFN induction by TLR3-independent pathways.

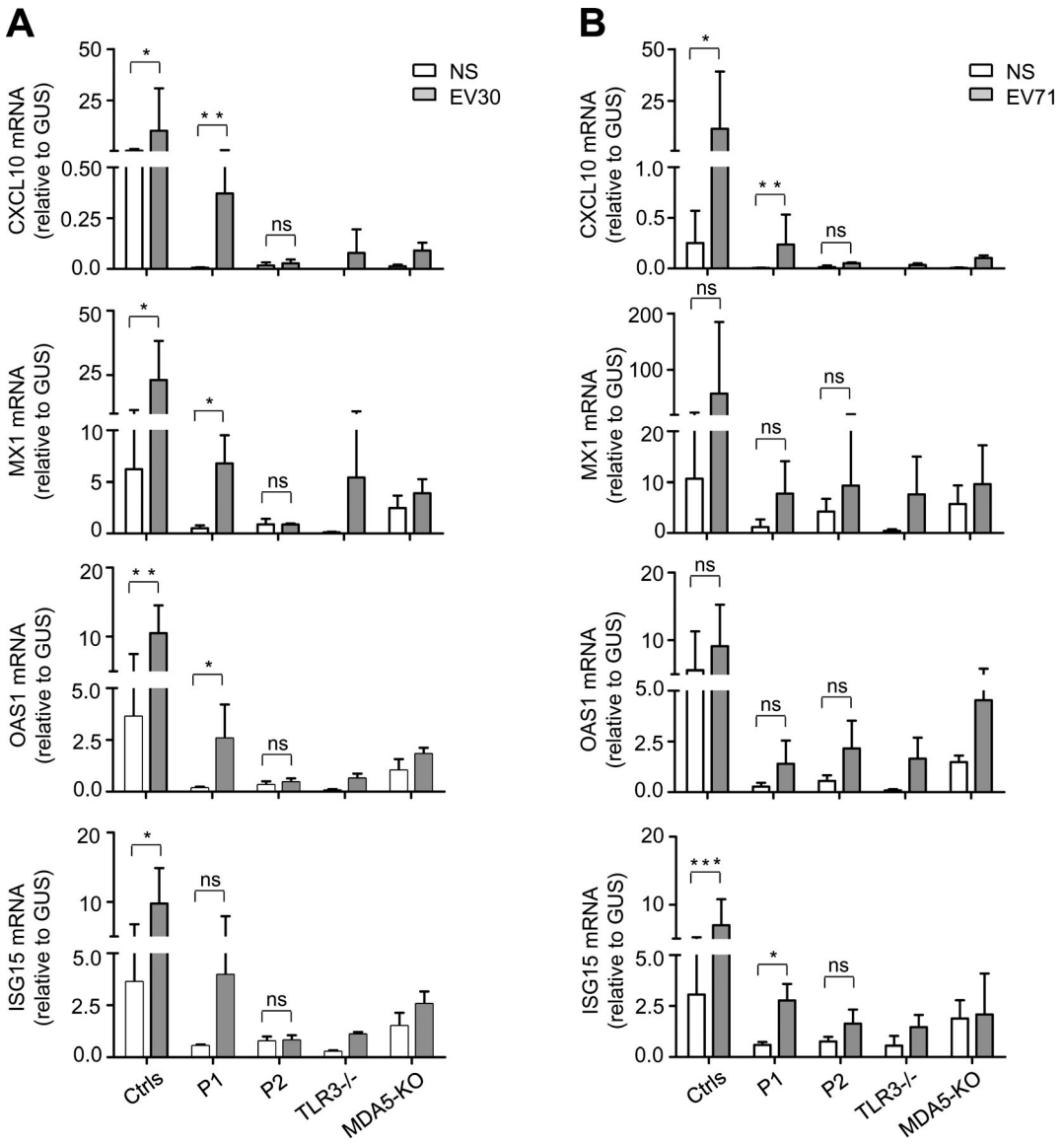

Figure S3. **ISG induction in TLR3- or MDA5-deficient fibroblasts following EV30 or EV71 infection. (A and B)** mRNA levels for *CXCL10*, *MX1*, *OAS1*, and *ISG15* in SV40-fibroblasts from three healthy controls (Ctrls), P1, P2, a *TLR3*$^{-/-}$ patient, and MDA5 KO SV40-fibroblasts, as quantified by RT-qPCR following 24 h of infection with EV30 (A) or EV71 (B) at an MOI of 5. Mean values ± SD were calculated from three independent experiments. P values were obtained by paired samples *t* test. ns, P > 0.05; *, P < 0.05; **, P < 0.01; ***, P < 0.001.

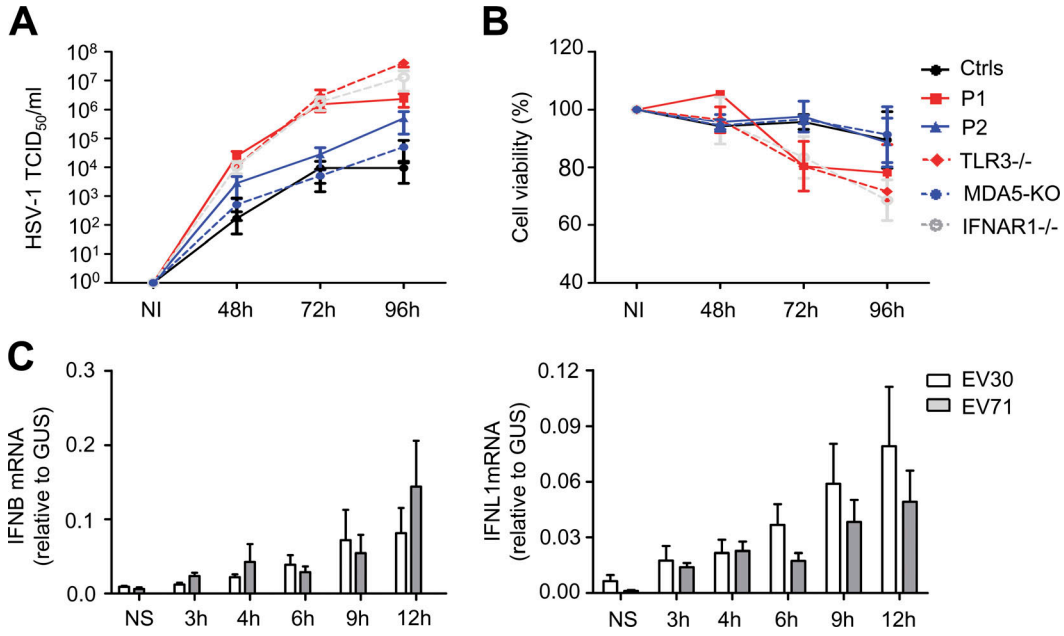

Figure S4. **Measurement of HSV-1 susceptibility and EV-induced IFN production in human SV40-fibroblasts. (A and B)** Levels of HSV-1 replication (A) and cell viability (B) were assessed for SV40-fibroblasts from three healthy controls (Ctrls), P1, P2, a *TLR3*$^{-/-}$ patient, MDA5 KO SV40-fibroblasts, and an *IFNAR1*$^{-/-}$ patient, at various time points after infection with HSV-1 at an MOI of 0.001. NI, not infected. **(C)** Levels of *IFNB* and *IFNL1* mRNA, in SV40-fibroblasts from one healthy control, at various time points after infection with EV30 or EV71 at an MOI of 5. NS, not stimulated. Mean values ± SD were calculated from three independent experiments (A–C).

Table S1 and Table S2 are provided online as separate files. Table S1 shows homozygous and compound heterozygous rare nonsynonymous variants in P1. Table S2 shows homozygous and compound heterozygous rare nonsynonymous variants in P2.